

# Organic & Biomolecular Chemistry

Accepted Manuscript



This is an *Accepted Manuscript*, which has been through the Royal Society of Chemistry peer review process and has been accepted for publication.

*Accepted Manuscripts* are published online shortly after acceptance, before technical editing, formatting and proof reading. Using this free service, authors can make their results available to the community, in citable form, before we publish the edited article. We will replace this *Accepted Manuscript* with the edited and formatted *Advance Article* as soon as it is available.

You can find more information about *Accepted Manuscripts* in the [Information for Authors](#).

Please note that technical editing may introduce minor changes to the text and/or graphics, which may alter content. The journal's standard [Terms & Conditions](#) and the [Ethical guidelines](#) still apply. In no event shall the Royal Society of Chemistry be held responsible for any errors or omissions in this *Accepted Manuscript* or any consequences arising from the use of any information it contains.

## Design, synthesis, conformational analysis and application of indolizidin-2-one dipeptide mimics

Cite this: DOI: 10.1039/x0xx00000x

Arkady Khashper<sup>a</sup> and William D. Lubell<sup>a</sup>

Received 00th January 2014,  
Accepted 00th January 2014

DOI: 10.1039/x0xx00000x

www.rsc.org/

Growth in the field of peptide mimicry over the past few decades has resulted in the synthesis of many new compounds and the investigation of novel pharmacological agents. Azabicyclo[X.Y.0]alkanone amino acids are among the attractive classes of constrained mimics, because they can create rigid peptide structures for probing the conformation and roles of natural motifs in recognition events important for biological activity. Herein, we review the last ten years of the synthesis, conformational analysis and activity of analogs of the azabicyclo[4.3.0]alkan-2-one amino acid subclass, so-called indolizidin-2-one amino acids, with particular attention on their employment as inputs for biological applications.



Dr. Arkady Khashper was born in 1969 in Ufa, Russia. He received his M.Sc. degree in Organic Synthesis from Ufa State Petroleum Technological University in 1993 and obtained his Ph.D. from the same university in 1998 in the area of Organic Chemistry under the supervision of Professor Kantor E.A. and Dr. Melnitsky I.A. In 2002, he joined the research group at FineTech Pharmaceuticals, Haifa, Israel. Since 2011, Dr. Khashper has been an Invited Researcher in the laboratory of Professor William D. Lubell in the Chemistry Department of the Université de Montréal, Canada. His scientific research interests focus on the synthesis of pharmaceutically active compounds, peptide mimetics, quantum-chemistry calculations and conformational analysis.

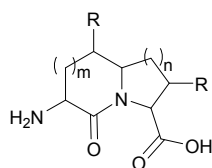


Dr. William D. Lubell received his Ph.D. in 1989 from the University of California, Berkeley under the supervision of Professor Henry Rapoport, and later studied as a postdoctoral fellow with Professor Ryoji Noyori at Nagoya University, Japan. In 1991, he joined the Chemistry Department of the Université de Montréal, where he is Full Professor. Advancing applications of peptides in drug discovery, Lubell has innovated methods for constraining amino acids and peptides to study structure-activity relationships and evolve peptidomimetic drug candidates with enhanced pharmacokinetic properties, including submonomer azapeptide synthesis, aminolactam scanning and azabicycloalkane amino acid libraries.

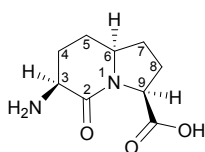
### 1. Introduction

Peptides have garnered notable interest in the last few decades due to their remarkable utility in various fields including medicine, materials science and nanotechnology.<sup>1</sup> Consequently, there has been parallel growth in approaches to mimic peptide structure and function in order to improve their properties and to gain understanding of their active conformers. Among various classes of peptidomimetics,<sup>2-11</sup> the azabicyclo[X.Y.0]alkanone amino acids (Figure 1) have been particularly well studied,<sup>12,13</sup> in great part because these rigid dipeptide surrogates can replicate turn conformations, which are ubiquitous in natural recognition events.<sup>14</sup> The design, synthesis and application of these constrained mimics have thus been particularly important for investigations to delineate

relationships between peptide conformation and biological activity. Indolizidin-2-one amino acids (I<sup>2</sup>aa), the azabicyclo[4.3.0]alkan-2-one subclass of these rigid dipeptides, have seen significant recent use in structure-activity relationship (SAR) studies of biologically relevant peptides and proteins, likely due to effective methods for synthesizing these challenging structures and their functionalized derivatives, as well as their effective capacity to replicate the dihedral angle geometry found in the backbones of ideal  $\beta$ - and  $\gamma$ -turn conformations (Figure 1). This review focuses on the design, synthesis, conformational analysis and biological activity of I<sup>2</sup>aa analogs with emphasis on their employment as inputs in peptidomimetics for chemical biology and medicinal chemistry studies.



Azabicyclo[X.Y.0]alkan-2-one amino acid



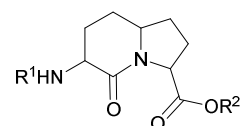
(3S,6S,9S)-1

**Figure 1.** Representative azabicyclo[X.Y.0]alkan-2-one amino acid and (3S,6S,9S)-Indolizidin-2-one amino acid [(3S,6S,9S)-1] with heterocycle numbering<sup>15</sup>.

## 2. Methods for the synthesis of indolizidinone amino acids

Earlier syntheses of the parent I<sup>2</sup>aa as well as substituted variants have been previously reviewed.<sup>12,13,16-18</sup> The reader should consult these earlier reviews for research conducted prior to 2004, which includes preparations of substituted I<sup>2</sup>aa analogs with substituents in positions 3, 4, 5, 7, and 8, as well as multi-substituted examples (itemized in Figures 2-4). In this review, I<sup>2</sup>aa syntheses performed after 2004 will be covered, including novel substituted systems and new synthetic routes to known compounds.

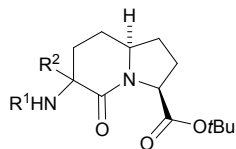
### Parent indolizidinones



- R<sup>1</sup> = H, R<sup>2</sup> = H (3S,6S,9S)-, (3S,6R,9S)-, (3R,6R,9R)-**1**<sup>12</sup> (3S,6S,9R)-**1**<sup>12,18</sup>  
 R<sup>1</sup> = Boc, R<sup>2</sup> = H (3S,6S,9S)-**2**<sup>12,16,18</sup> (3S,6R,9S)-**2**<sup>12,16</sup>  
 R<sup>1</sup> = Cbz, R<sup>2</sup> = H (3S,6S,9S)-, (3R,6R,9S)-**3**<sup>12</sup>  
 R<sup>1</sup> = Boc, R<sup>2</sup> = Me (3S,6S,9S)-, (3S,6R,9S)-**4**<sup>12,13,16</sup> (3S,6S,9R)-**4**<sup>13,16</sup>  
 R<sup>1</sup> = Cbz, R<sup>2</sup> = Me (3S,9S)-, (3R,9S)-**5**<sup>13</sup>  
 R<sup>1</sup> = Cbz, R<sup>2</sup> = Et (3S,6S,9S)-, (3R,6S,9S)-**6**<sup>18</sup>  
 R<sup>1</sup> = Boc, R<sup>2</sup> = *t*Bu (3S,6S,9S)-, (3S,6R,9S)-, (3R,6S,9S)-, (3R,6R,9S)-**7**<sup>13,17</sup>  
 R<sup>1</sup> = Ac, R<sup>2</sup> = *t*Bu (3S,6S,9S)-, (3R,6S,9S)-**8**<sup>17</sup>

**Figure 2.** Representative examples of previously reviewed parent I<sup>2</sup>aa and their protected variants with citations to reviews in which further information on their synthesis and use may be obtained.

## Mono-substituted indolizidinones



$R^1 = H, R^2 = Bn$  (3*R*)-**9**<sup>17,18</sup>

$R^1 = H, R^2 = 1\text{-Naphthyl}$  (3*R*)-**10**<sup>17,18</sup>

$R^1 = H, R^2 = 2\text{-Naphthyl}$  (3*R*)-**11**<sup>17,18</sup>

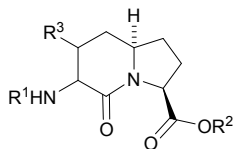
$R^1 = Ac, R^2 = Me$  (3*S*)-**12**<sup>18</sup>

$R^1 = Ac, R^2 = Et$  (3*S*)-**13**<sup>18</sup>

$R^1 = Ac, R^2 = Bn$  (3*R*)-**14**<sup>17,18</sup>

$R^1 = Bn, R^2 = Bn$  (3*S*)-, (3*R*)-**15**<sup>18</sup>

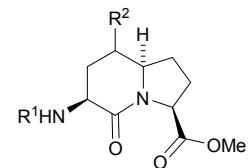
$R^1 = Bn, R^2 = \text{allyl}$  (3*S*)-, (3*R*)-**16**<sup>18</sup>



$R^1 = H, R^2 = Me, R^3 = Ph$  (3*S,4R*)-**17**<sup>13</sup>

$R^1 = Ac, R^2 = tBu, R^3 = Me$  (3*S,4S*)-, (3*R,4R*)-**18**<sup>17</sup>

$R^1 = Ac, R^2 = tBu, R^3 = Ph$  (3*S,4R*)-, (3*R,4S*)-**19**<sup>17</sup>



$R^1 = Boc, R^2 = Me$  (5*S*)-**20**<sup>13</sup>

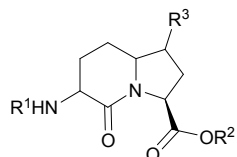
$R^1 = Boc, R^2 = Bn$  (5*S*)-, (5*R*)-**21**<sup>13,16</sup>

$R^1 = Boc, R^2 = CH_2OH$  (5*S*)-**22**<sup>13,16</sup>

$R^1 = Boc, R^2 = COH$  (5*S*)-**23**<sup>13,16</sup>

$R^1 = Boc, R^2 = CO_2H$  (5*S*)-**24**<sup>13,16</sup>

$R^1 = Phth, R^2 = CH_2Cl$  (5*S*)-, (5*R*)-**25**<sup>18</sup>



$R^1 = H, R^2 = H, R^3 = CH_2NH_2$  (3*S,6S,7S*)-**26**<sup>18</sup>

$R^1 = H, R^2 = H, R^3 = CO_2H$  (3*S,6S,7R*)-**27**<sup>18</sup>

$R^1 = H, R^2 = H, R^3 = \text{allyl}$  (3*S,6S,7R*)-**28**<sup>18</sup>

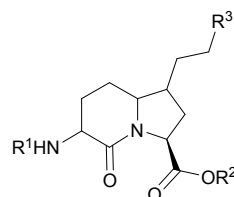
$R^1 = Boc, R^2 = Me, R^3 = Me$  (3*S,6S,7R*)-**29**<sup>13,16</sup>

$R^1 = Boc, R^2 = Me, R^3 = CH_2N_3$  (3*S,6S,7S*)-**30**<sup>13</sup>

$R^1 = Boc, R^2 = Me, R^3 = CH_2OH$  (3*S,6S,7R*)-, (3*S,6R,7R*)-**31**<sup>13,16</sup>

$R^1 = Boc, R^2 = Me, R^3 = Bn$  (3*S,6S,7R*)-, (3*S,6R,7S*)-**32**<sup>13,16</sup>

$R^1 = Cbz, R^2 = Et, R^3 = Bn$  (3*S,6S,7R*)-, (3*R,6S,7R*)-**33**<sup>13</sup>



$R^1 = H, R^2 = H, R^3 = CH_2NH_2$  (3*S,6S,7R*)-**34**<sup>18</sup>

$R^1 = Boc, R^2 = H, R^3 = CH_2N_3$  (3*S,6S,7R*)-**35**<sup>13</sup>

$R^1 = Boc, R^2 = Me, R^3 = CH_2N_3$  (3*S,6S,7R*)-**36**<sup>13</sup>

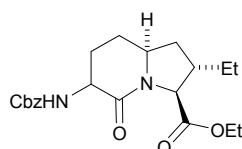
$R^1 = Boc, R^2 = Me, R^3 = CH_2OTBDMS$  (3*S,6S,7R*)-**37**<sup>13</sup>

$R^1 = Boc, R^2 = tBu, R^3 = OTDS$  (3*S,6R,7R*)-, (3*R,6R,7R*)-**38**<sup>17</sup>

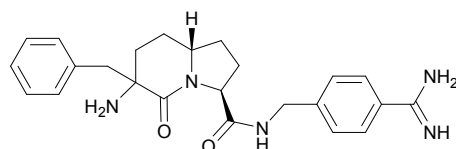
$R^1 = Boc, R^2 = tBu, R^3 = OTBDMS$  (3*R,6R,7R*)-**39**<sup>13</sup>

$R^1 = Cbz, R^2 = Et, R^3 = OH$  (3*S,6S,7S*)-, (3*R,6S,7S*)-**40**<sup>18</sup>

$R^1 = Cbz, R^2 = Et, R^3 = N_3$  (3*S,6S,7R*)-, (3*R,6S,7R*)-**41**<sup>18</sup>



(3*S*)-, (3*R*)-**42**<sup>13</sup>



**43**<sup>13,18</sup>

**Figure 3.** Representative examples of previously reviewed mono-substituted  $l^2$  aas with citations to reviews in which further information on their synthesis and use may be obtained.

## Multi-substituted indolizidinones

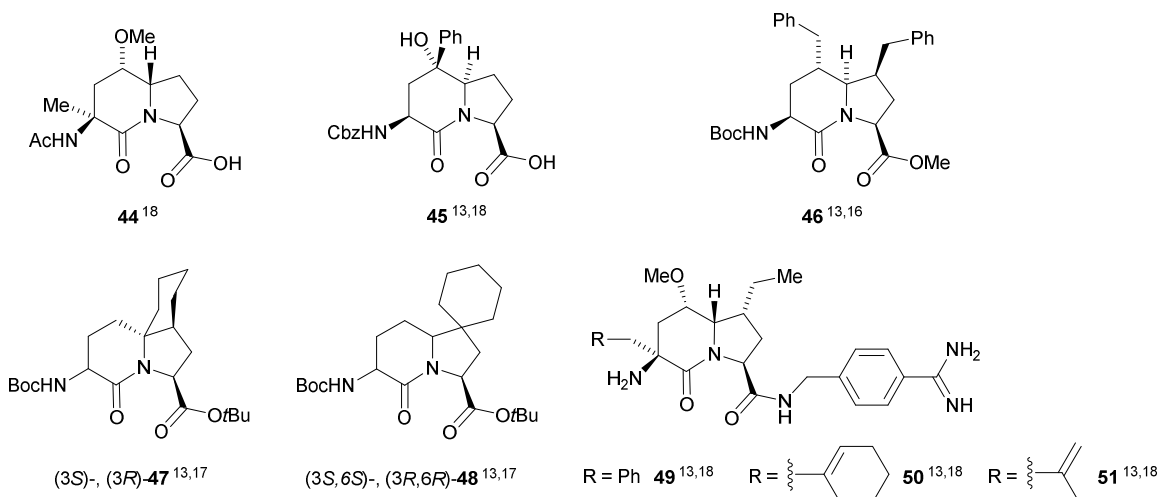
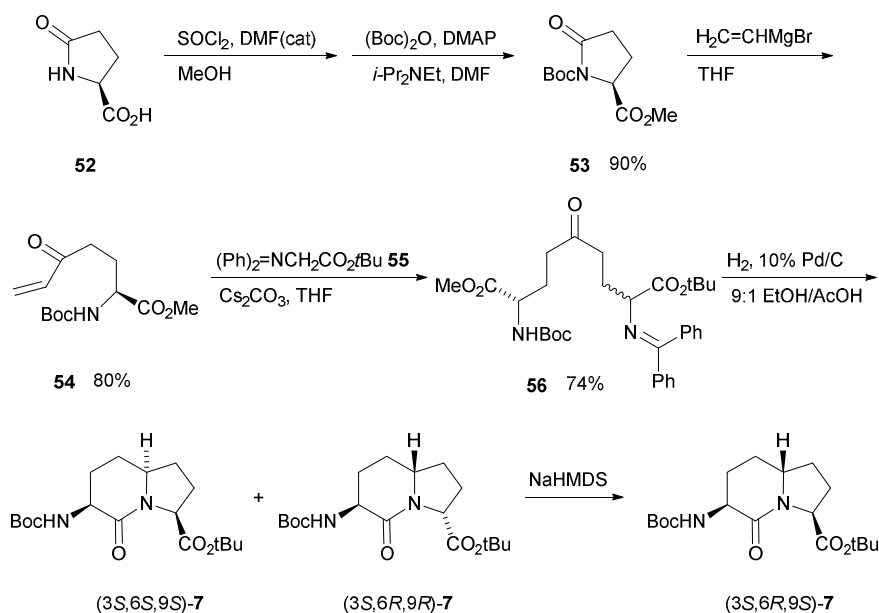


**Figure 4.** Representative examples of previously reviewed multi-substituted I<sup>2</sup>aas with citations to reviews in which further information on their synthesis and use may be obtained.

### 2.1. Synthetic methods for the construction of the parent indolizidinone amino acid

Diastereomeric (3*S*)-I<sup>2</sup>aas, (6*S*,9*S*)-, (6*R*,9*R*)- and (6*R*,9*S*)-7 were prepared from pyrrolidone **52** by a route featuring reductive amination and lactam cyclization from 5-oxo-2,8-diamino azelate **56** (Scheme 1).<sup>19</sup> Ring opening of pyrrolidone **53** with vinylmagnesium bromide gave  $\alpha,\beta$ -unsaturated ketone **54**. Conjugate addition of glycine enolate **55**

to enone **54** gave an equimolar inseparable mixture of diastereomeric azelates **56**, which was used directly in the cyclization sequence. High stereoselectivity for the *cis*-diastereomer of the 5-substituted proline provided access to the (3*S*,6*S*,9*S*)- and (3*S*,6*R*,9*R*)-indolizidinones **7**, which were separated by silica gel chromatography. Epimerization of the (3*S*,6*R*,9*R*)-isomer with sodium hexamethyldisilazide gave access to (3*S*,6*R*,9*S*)-indolizidinone **7**.

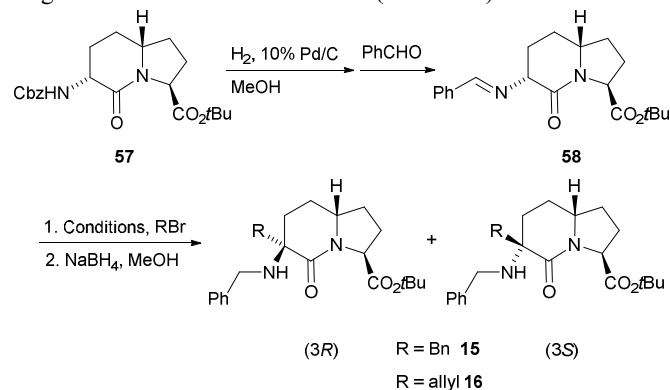


**Scheme 1.** Synthesis of 3-*N*-(Fmoc)amino-azabicyclo[4.3.0]nonane-9-carboxylate diastereomers **7**.

### 2.2. Synthesis of mono-substituted indolizidinone amino acid derivatives

Alkylation of Schiff base **58** using benzyl and allyl bromides produced different ratios of 3*R*/3*S*-diastereomers (from 92:8 to 2:98), contingent on base and conditions favoring respectively the 3*R* (9:1) and 3*S* (2:98) diastereomers using lithium

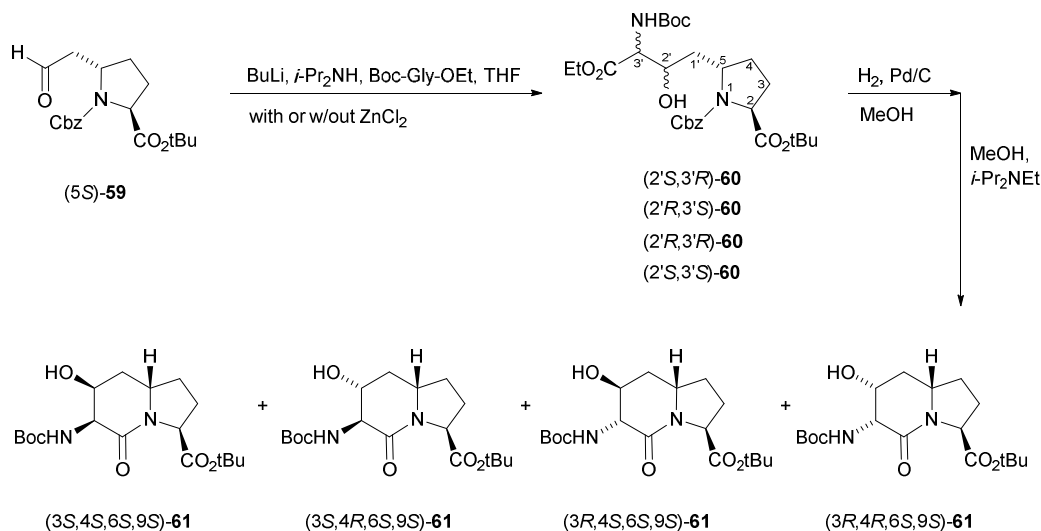
hexamethyldisilazide in the absence and presence of magnesium bromide as Lewis acid (Scheme 2).



**Scheme 2.** Synthesis of 3-*N*-benzylamino-3-benzyl- and 3-allyl-indolizidin-2-one carboxylates.

After imine reduction with NaBH<sub>4</sub>, the corresponding 3-*N*-benzylamino-3-alkyl-indolizidin-2-one carboxylate diastereomers of **15** and **16** were separated. The pure isomers (3*S*)-**15** and (3*R*)-**16** were obtained by recrystallization from ethyl ether.<sup>20,21</sup>

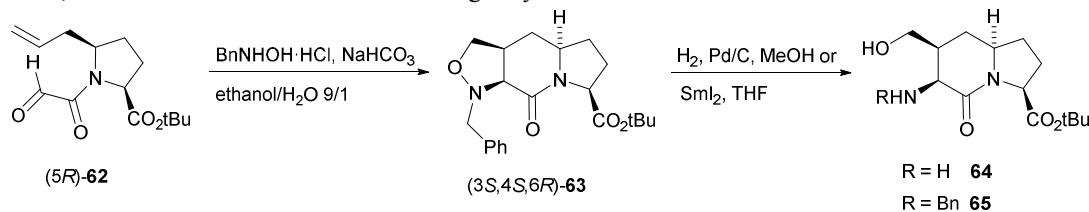
Constrained Ser-Pro dipeptide mimics, 4-hydroxyindolizidinones **61** were synthesized by a route featuring aldol condensation of pyroglutamate-derived aldehyde (5*S*)-**59** with the enolate of ethyl Boc-glycinate, and lactam cyclization (Scheme 3).<sup>22</sup> Employing lithium diisopropylamide and ZnCl<sub>2</sub> in the aldol condensation gave all four diastereomers in equimolar amounts; however, after lactam formation the diastereomers could be separated by purification by flash chromatography. Similarly, four more diastereomeric 4-hydroxyindolizidinones **61** were prepared using an analogous route from the diastereomeric aldehyde (5*R*)-**59**.



**Scheme 3.** Aldol route to 4-hydroxy-indolizidin-2-ones **61**.

Constrained homoSer-Pro mimics were prepared by a route featuring a 1,3-dipolar cycloaddition.<sup>23</sup> The intramolecular reaction of the nitron obtained from treating diastereomeric *N*-oxoacetyl-5-allylprolines (5*R*)- and (5*S*)-**62** with *N*-benzylhydroxylamine provided stereoselectively the fused isoxazolindines **63**, which underwent reductive cleavage by

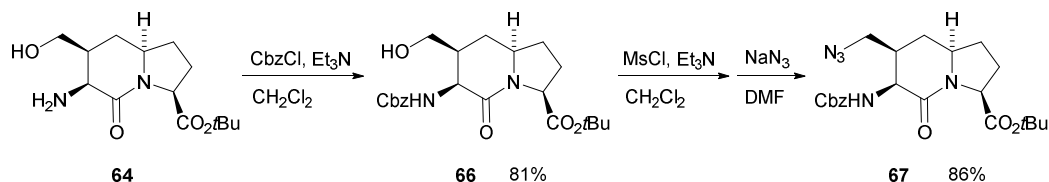
hydrogenolysis with hydrogen and palladium-on-carbon or by samarium iodide to provide respectively 3-amino or 3-*N*-benzylamino 4-hydroxymethyl indolizidin-2-one carboxylates **64** and **65** (Scheme 4).



**Scheme 4.** 1,3-Dipolar cycloaddition route to 3-amino- and 3-benzylamino-4-hydroxymethylindolizidin-2-one-9-carboxylates **64** and **65**.

The hydroxyl group of **64** has served as gateway for adding other functions at the I<sup>2</sup>aa 4-position. For example, the azidomethyl analog was prepared from **64** in three steps by

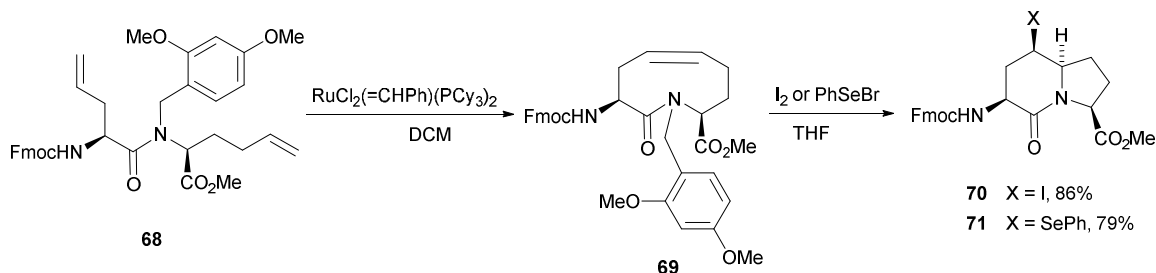
amine protection, activation as the methanesulfonate and displacement by heating with sodium azide in DMF at 80°C (Scheme 5).<sup>24</sup>



**Scheme 5.** Synthesis of 3-*N*-(Cbz)amino-4-azidomethylindolizidin-2-one-9-carboxylate **67**.

A ring-closing metathesis / electrophilic transannular cyclization route to azabicycloalkanone amino acids has proven particularly effective for producing a variety of fused 6,5- and 7,5-ring systems with control of stereochemistry.<sup>25-27</sup> For example, 3-*N*-(Fmoc)amino-5-iodo- and 5-phenylselenyl-indolizidin-2-one-9-carboxylates **70** and **71** were stereoselectively prepared from routes employing *N*-(Fmoc)allyllycylglycyl-*N*-(dimethoxybenzyl)homoallylglycine **68**

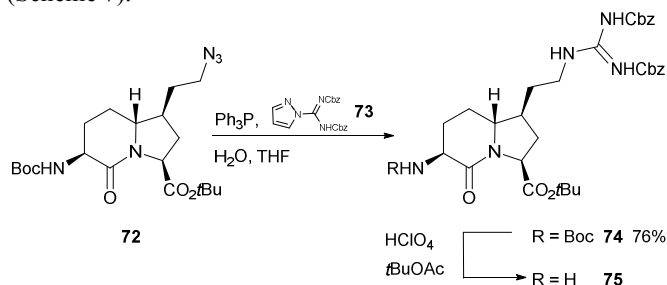
(Scheme 6). Ring-closing metathesis on **68** provided the *Z*-olefin in 9-membered macrocyclic dipeptide **69**,<sup>28</sup> which on treatment with iodine or diphenylselenide gave respectively **70** and **71** as single diastereomers. Alternatively, removal of the dimethoxybenzyl group prior to cyclization gave a 2:1 ratio of (5*R*,6*S*)- and (5*S*,6*R*)-iodides **70**.



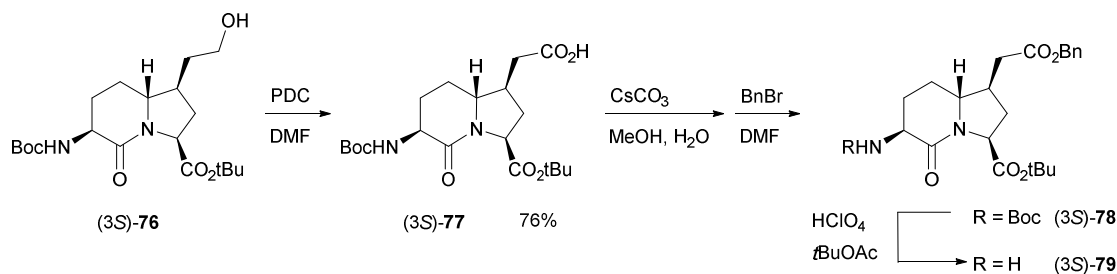
**Scheme 6.** Ring-closing metathesis / electrophilic transannular cyclization route to 5-substituted indolizidin-2-one amino acids **70** and **71**.

Constrained Gly-Arg analog **74** was synthesized employing azide **72**,<sup>29</sup> using a one-pot reduction/guanidinylation sequence (Scheme 7).<sup>30</sup>

Diastereomeric, constrained Gly-Asp analogs (3*S*)- and (3*R*)-**79** were prepared from the respective 7-hydroxyethyl I<sup>2</sup>aa derivative **76**,<sup>30</sup> by a route featuring oxidation with pyridinium dichromate (PDC), followed by carboxylate protection through alkylation of the corresponding cesium salt with benzyl bromide (Scheme 8).<sup>30</sup>



**Scheme 7.** Synthesis of 3-amino-7-guanidinoethylindolizidin-2-one-9-carboxylate **75**.



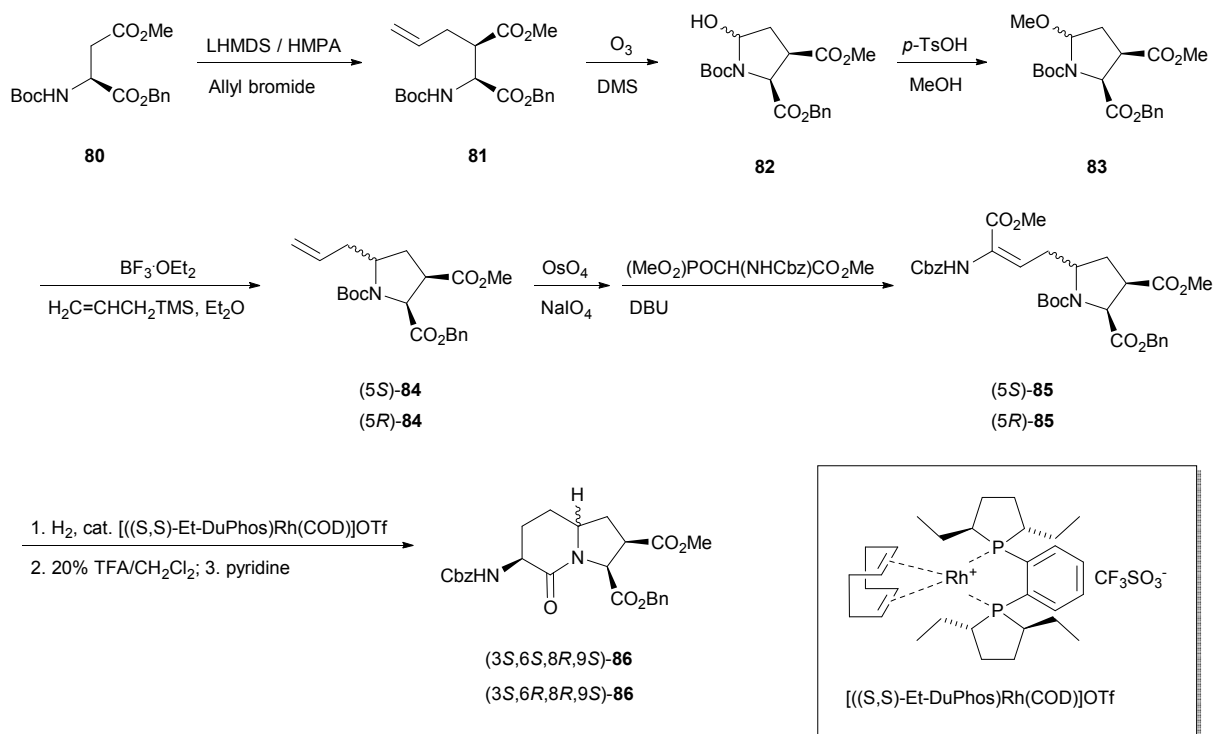
**Scheme 8.** Carboxylate introduction at the I<sup>2</sup>aa 7-position.

Diastereomeric constrained Nle-Asp dipeptide mimics **86** were synthesized using a multistep sequence from (2*S*)-*N*-

(Boc)aspartate **80** (Scheme 9).<sup>31</sup> Alkylation of the enolate of **80** provided the  $\beta$ -allyl aspartate **81** in a total yield of 57% and a

diastereomeric ratio of 4:1 in favor of the (2*S*,3*R*)-isomer. Ozonolysis of (2*S*,3*R*)-**81** and allylation of the resulting cyclic hemi-aminal **82** gave a 1:1 mixture of diastereomeric 5-allyl prolines **84**. Ozonolysis of (2*S*,3*R*)-**84** followed by Horner-Emmons olefination onto the resulting aldehyde gave protected

dehydroamino ester **85**. Hydrogenation with a chiral catalyst, and lactam cyclization provided 3-amino-indolizidin-2-one-8,9-dicarboxylate **86** (Scheme 9).

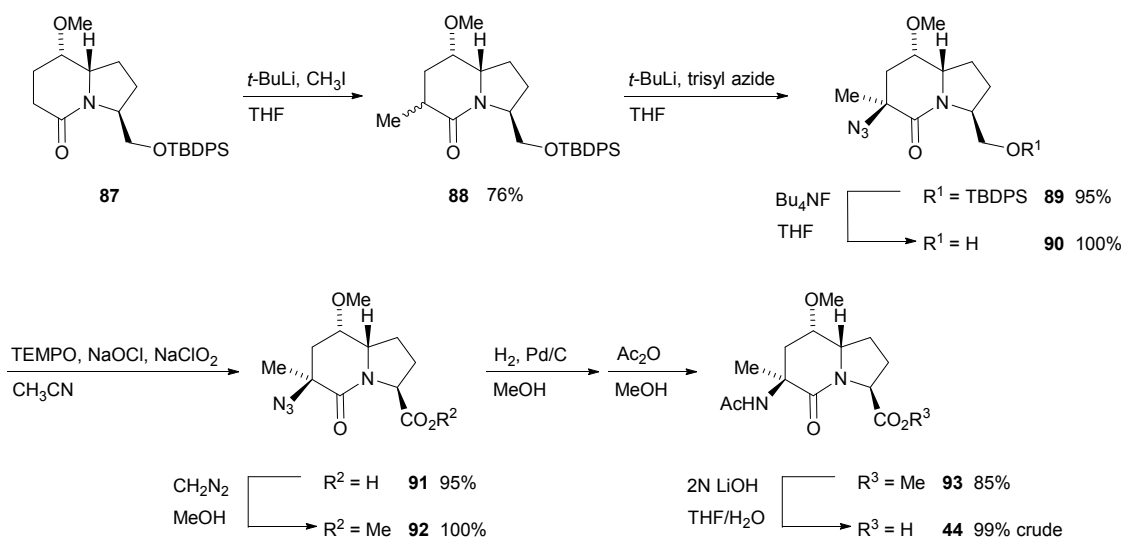


Scheme 9. Synthesis of 3-amino-indolizidin-2-one-8,9-dicarboxylate **86**.

### 2.3. Synthesis of multi-substituted indolizidinone amino acid derivatives

(3*S*,5*S*,6*S*,9*S*)-3-Methyl-5-methoxy-indolizidin-2-one scaffold **44** was synthesized from bicyclic lactam **87**,<sup>32</sup> derived from *S*-

pyroglutamic acid.<sup>33</sup> Enolization of the lactam with *tert*-butyl lithium was sequentially used to install methyl and azide groups to provide the quaternary center of **89** with high diastereoselectivity. Oxidation of alcohol **90**, azide reduction and *N*-acetylation furnished amido acid **44** (Scheme 10).



Scheme 10. Synthesis of 3-methyl-5-methoxy-1,2,3,4-tetrahydroindolizidin-2-one derivative **44**.

### 3. Conformational analysis of indolizidinone peptide analogs

The effective application of indolizidin-2-one amino acid analogues to prepare mimics that replicate the form and function of natural peptides requires understanding of their preferred conformations alone and in peptide structures. Spectroscopic, computational and crystallographic analyses

have provided insight into the influences of neighboring sequences, ring substituents, and stereochemistry.<sup>34-36</sup>

#### 3.1. Analysis by NMR spectroscopy and computational methods

The influence of I<sup>2</sup>aa ring stereochemistry on conformation was examined in the protected cyclic penta-peptide *cyclo*-[Arg(Pmc)-Gly-Asp(OtBu)-I<sup>2</sup>aa] **94** using a combination of NMR spectroscopy in chloroform, as well as molecular mechanics and dynamic calculations (Figure 5).<sup>37</sup>

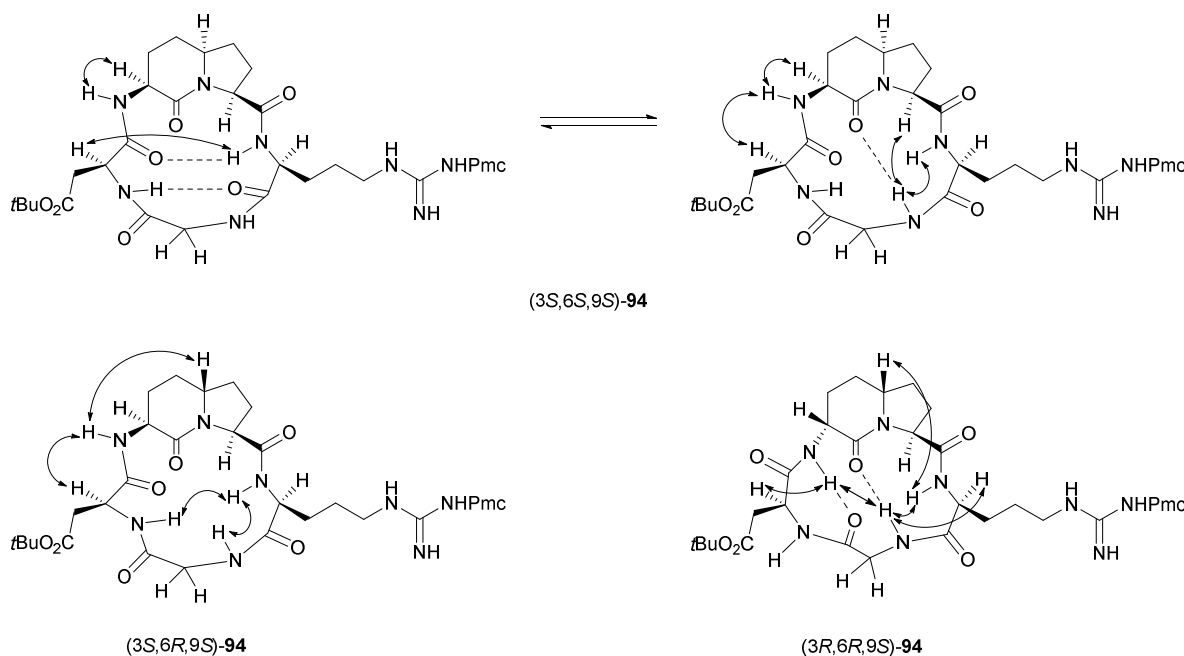


Figure 5. Significant hydrogen bonds and magnetization transfer in preferred conformers for **94**.

Amide protons engaged in intramolecular hydrogen bonds were ascertained by measuring their chemical shifts and temperature coefficients ( $\Delta\delta/\Delta T$ ). Protons nearby to one another were assessed by NOESY spectroscopy. In the case of the cyclic peptide containing (3*S*,6*S*,9*S*)-I<sup>2</sup>aa [(3*S*,6*S*,9*S*)-**94**], an equilibrium was observed between a conformer exhibiting  $\beta$ - and  $\gamma$ -turns centered respectively on the I<sup>2</sup>aa and glycine residues, and a second conformer in which the I<sup>2</sup>aa residue adopts the *i* and *i*+1 positions of a  $\beta$ -turn, in which a hydrogen bond was observed between the lactam carbonyl oxygen and glycine N-H (Figure 5). In contrast, the cyclic peptide possessing the convex (3*S*,6*R*,9*S*)-I<sup>2</sup>aa structure, diastereomer [(3*S*,6*R*,9*S*)-**94**], was not observed by NMR spectroscopy to adopt a specific conformer. Examination of the cyclic peptide bearing the (3*R*,6*R*,9*S*)-I<sup>2</sup>aa isomer, [(3*R*,6*R*,9*S*)-**94**], detected a major conformer in which the lactam carbonyl oxygen and C3-amine N-H of the I<sup>2</sup>aa residue were respectively engaged in  $\beta$ - and  $\gamma$ -turn hydrogen bonds with the N-H and the carbonyl of the glycine residue.<sup>37</sup>

Employing similar spectroscopic techniques, the unprotected cyclic peptide was examined in water. The (3*S*,6*S*,9*S*)-I<sup>2</sup>aa analog *cyclo*-[Arg-Gly-Asp-I<sup>2</sup>aa] **95** exhibited NOE shared between the amide N-H protons of the Asp and I<sup>2</sup>aa residues suggesting that both faced inside the penta-peptide ring. The N-H of the I<sup>2</sup>aa residue was engaged in a hydrogen bond with the carbonyl oxygen of the Arg residue in a  $\beta$ -turn centered on the

Gly-Asp residues (Figure 6).<sup>38</sup> To study the receptor bound conformer of **95**, transfer-NOE (trNOE) NMR spectroscopy was employed in the presence of human platelets to detect both NOE within the cyclic peptide and between this ligand and its protein receptor, which was assumed to be the  $\alpha_3\beta_3$  integrin receptor for which it exhibited affinity (154 nM).<sup>38</sup> In the trNOE experiment in the platelet suspension, new cross-peaks were observed indicative of a change in conformation relative to **95** in water. The “receptor-bound” conformation of **95** exhibited NOE characteristic of a  $\gamma$ -turn centered on the Asp residue.<sup>38</sup>

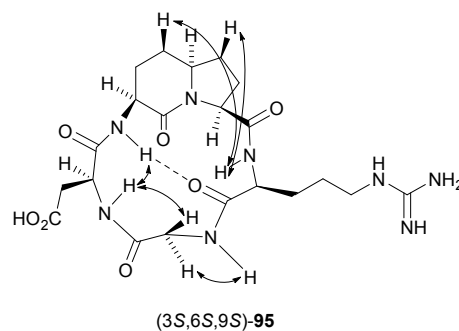


Figure 6. Significant long-range NOE contacts of **95** in H<sub>2</sub>O/D<sub>2</sub>O solution.

Employing Monte Carlo/stochastic dynamics (MC/SD) simulations using a generalized Born/surface area (GB/SA) solvation model for water, the conformations of cyclic Arg-Gly-Asp mimics containing the (3*S*, 4*S*, 6*R*, 9*S*)- and (3*R*, 4*R*, 6*S*, 9*S*)-4-hydroxymethyl indolizidinone amino acids (3*S*, 4*S*, 6*R*, 9*S*)- and (3*R*, 4*R*, 6*S*, 9*S*)-**96** were examined and found to adopt similar conformations as those observed using NMR spectroscopy and computational analysis on the parent I<sup>2</sup>aa systems described above. In particular, the cyclic peptide possessing the most activity in the series (IC<sub>50</sub> = 53.7±17.3 nM for α<sub>v</sub>β<sub>3</sub>), (3*R*, 4*R*, 6*S*, 9*S*)-**96** adopted a major conformer in which Arg sat at the *i*+2 position of a β-turn and Asp adopted the *i*+1 position of a γ-turn (Figure 7).<sup>39</sup> Docking of (3*R*, 4*R*,

6*S*, 9*S*)-**96** into a crystal structure of the extracellular segment of integrin α<sub>v</sub>β<sub>3</sub> gave a similar backbone conformer as that exhibited in the solvation model for water; the β-carboxylate side-chain of the Asp residue was coordinated to the metal cation in the metal-ion-dependent adhesion site and the hydroxyl methyl group of the I<sup>2</sup>aa residue sat outside of the integrin binding site. The similarity between the models of (3*R*, 4*R*, 6*S*, 9*S*)-**96** in water and bound to the integrin receptor suggested that the constraint of the I<sup>2</sup>aa residue created a pre-organized conformation for binding, which accounted for its high receptor affinity.<sup>39</sup>

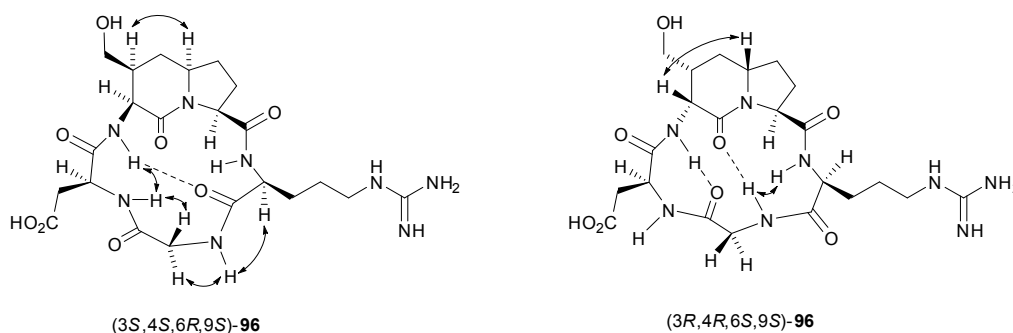


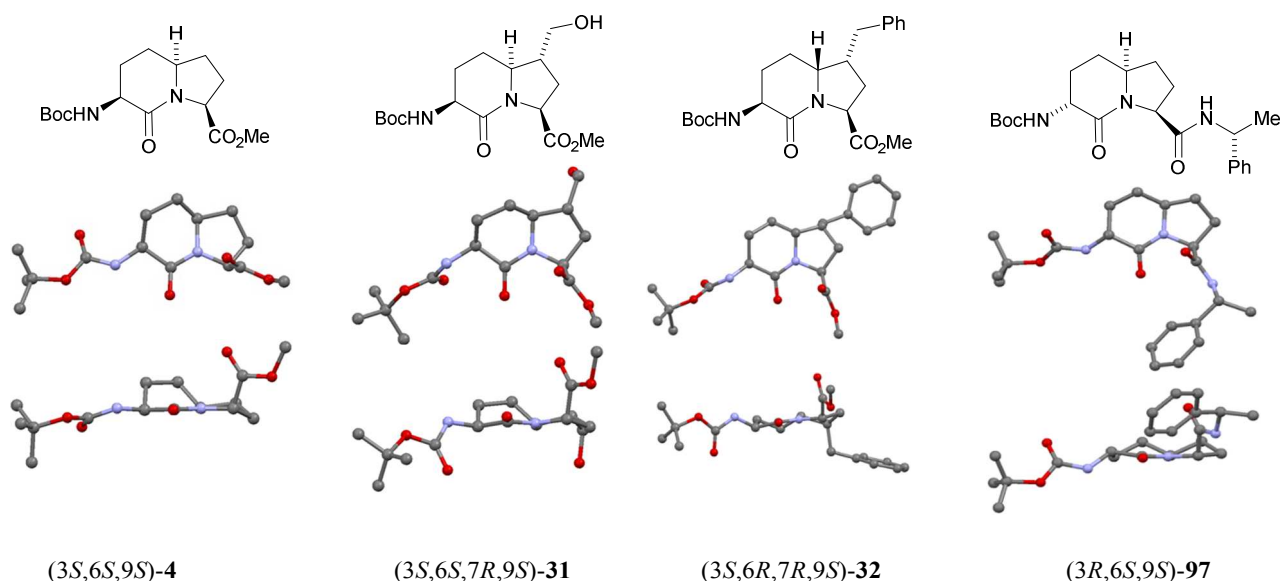
Figure 7. Long-range NOE contacts of (3*S*, 4*S*, 6*R*, 9*S*)- and (3*R*, 4*R*, 6*S*, 9*S*)-**96** in H<sub>2</sub>O/D<sub>2</sub>O.

On a different examination of the influence of (3*S*, 6*S*, 9*S*)-I<sup>2</sup>aa, a combination of 3D NMR experiments and molecular modeling indicated that the bicyclic mimic at the C-terminus of endothelin analogs did not induce a turn conformation in the linear peptide.<sup>40</sup>

### 3.2. Crystal structure data

In the reviewed period, crystallographic analyses have been reported for a set of four I<sup>2</sup>aa analogs: **97**,<sup>41</sup> (3*S*,6*R*)-**15**,<sup>21</sup> (3*S*,6*S*)-**15** and (3*R*,6*S*)-**16**<sup>20</sup>. For a visual aid to compare the structural factors (e.g., ring stereochemistry and ring

substituents) that influence conformation, images derived from the X-ray crystallographic analyses are presented with those for (3*S*,6*S*,9*S*)-methyl *N*-(Boc)amino indolizidin-2-one 9-carboxylate **4**, 7-hydroxymethyl I<sup>2</sup>aa (3*S*,6*S*,7*R*,9*S*)-**31** and 7-benzyl I<sup>2</sup>aa (3*S*,6*R*,7*R*,9*S*)-**32** in two perspectives, in which the ring system is placed facing and perpendicular to the viewer (Figure 8). In addition, the dihedral angles of the dipeptide embedded in the heterocyclic systems of these structures are compared with those of natural peptide secondary structures, such as the central residues in an ideal type II' β-turn (Table 1).



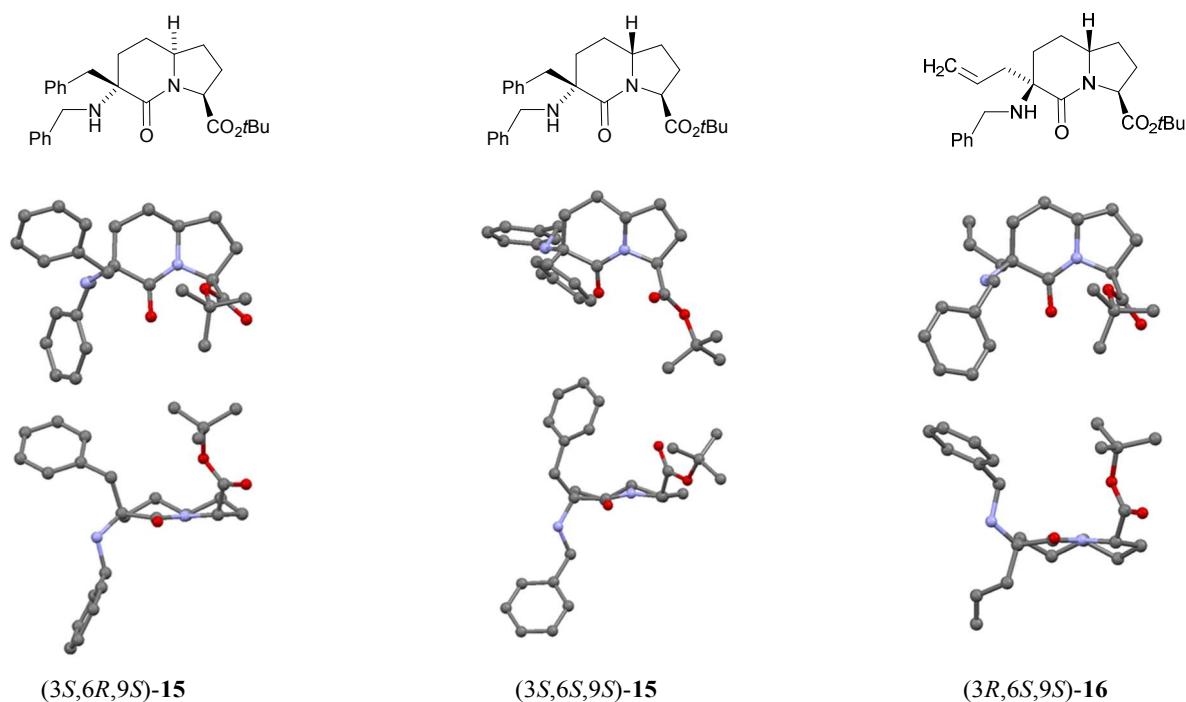
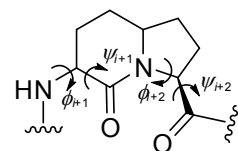


Figure 8. Crystallographic structures of I<sup>2</sup>aa analogs.

Table 1. Torsional angles of different I<sup>2</sup>aas from X-ray data and ideal secondary structures.



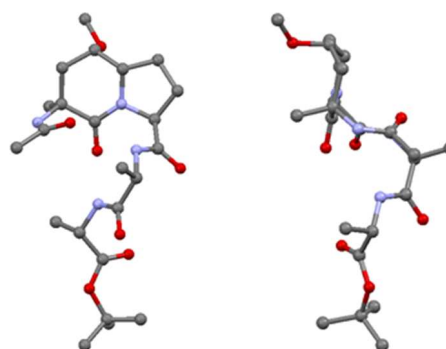
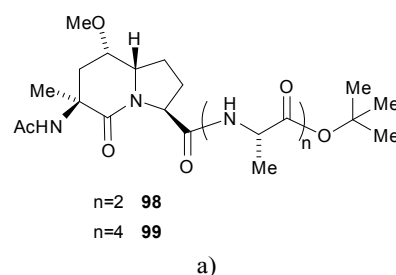
Entry	$\Phi_{i+1}, ^\circ$	$\Psi_{i+1}, ^\circ$	$\Phi_{i+2}, ^\circ$	$\Psi_{i+2}, ^\circ$	Ref.
II' $\beta$ -turn	60	-120	-80	0	42
inverse $\gamma$ -turn			-80	80	43
(3 <i>S</i> ,6 <i>S</i> ,9 <i>S</i> )-4	-159	-176	-78	179	34
(3 <i>S</i> ,6 <i>S</i> ,7 <i>R</i> ,9 <i>S</i> )-31	-82	-175	-68	151	36
(3 <i>S</i> ,6 <i>R</i> ,7 <i>R</i> ,9 <i>S</i> )-32	-123	-147	-56	129	35
(3 <i>S</i> ,6 <i>R</i> ,9 <i>S</i> )-15	-61	139	-61	-23	21
(3 <i>S</i> ,6 <i>S</i> ,9 <i>S</i> )-15	-67	126	-70	151	20
(3 <i>R</i> ,6 <i>S</i> ,9 <i>S</i> )-16	58	-128	-64	-38	20
(3 <i>R</i> ,6 <i>S</i> ,9 <i>S</i> )-97	159	143	-56	145	41
(3 <i>S</i> ,5 <i>S</i> ,6 <i>S</i> ,9 <i>S</i> )-98	54	-127	-61	-23	32

Note: Atomic coordinates obtained from the Cambridge Crystallographic Data Center

Examining the X-ray data, the changes in the configuration of the peptide backbone have significant effects on dihedral angle values as they do in natural peptides. Focusing on the dihedral angles  $\psi^{i+1}$  and  $\phi^{i+2}$  constrained within the bicyclic system, because they may be the least influenced by crystal packing forces, the ring-fusion stereochemistry and the ring substituents have relatively less significant effects than those of the backbone stereocenters. For example, the proline  $\phi^{i+2}$  dihedral angle changes only  $\pm 22$  degrees on modification of the ring-fusion stereochemistry and the ring substituents. The  $\delta$ -lactam  $\psi^{i+1}$  dihedral angle varies by  $\pm 49$  degrees with apparently more

significant effects coming from ring-fusion stereochemistry than substituents.

Attachment of (3*S*,5*S*,6*S*,9*S*)-3-acetamido-3-methyl-5-methoxy-indolizidin-2-one-9-carboxylic acid **44** to di- and tetra-alanine *tert*-butyl esters provided peptides **98** and **99**, which were shown to adopt 3<sub>10</sub>-helical arrangements by NMR and CD spectroscopy in CDCl<sub>3</sub>. The acetamide and lactam carbonyl oxygen of **44** were found to engage respectively in ten-member  $\beta$ -turn hydrogen bonds with alanine N–H residues as confirmed by X-ray crystallography of the peptide **98**. This turn-turn conformation nucleates a longer 3<sub>10</sub>-helix in **99** (Figure 9).<sup>32</sup>



b)

**Figure 9.** a) Di- and tetraalanine I<sup>2</sup>aa peptides **98** and **99**; b) I<sup>2</sup>aa **98** face and side views.

The side view of compound **98** illustrates that the 6- and 5-membered heterocycles, both are in an envelope conformation with seven atoms [1-4, 6, 8-9] all in the same plane.

#### 4. Applications of indolizidinone amino acids.

##### Synthesis and Biological Activity of Receptor Ligands and Enzyme Inhibitors

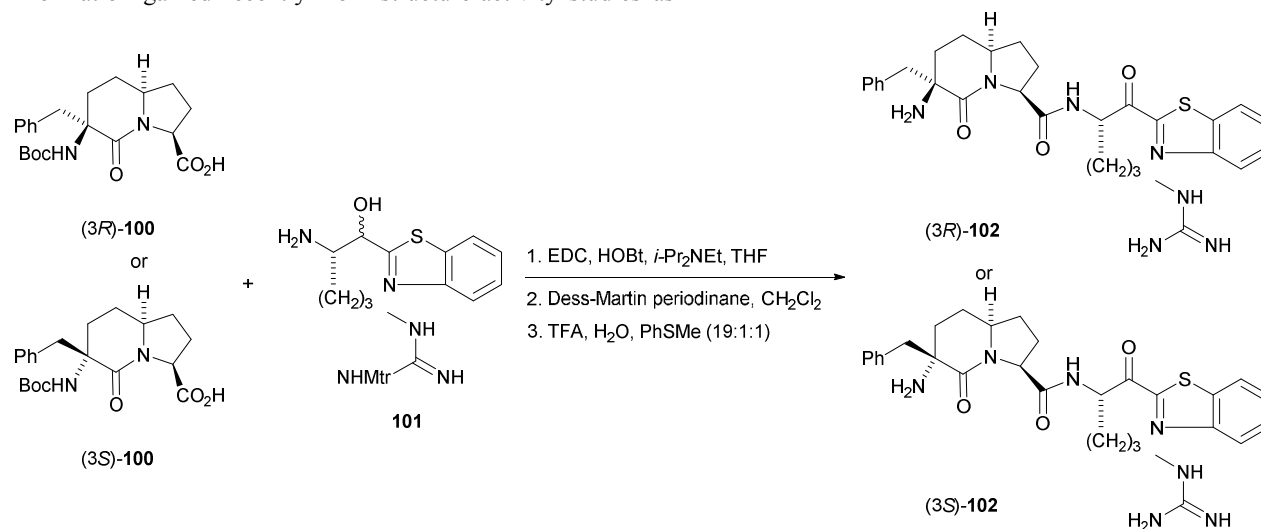
Peptide secondary structures, such as helices and turn motifs, have been implicated as recognition elements in a variety of biological interactions.<sup>14,44-47</sup> In efforts to understand their biologically active conformers and to transform peptide leads into small molecule drug candidates, the design and synthesis of constrained mimics of turn structures have been investigated. From this point of view, the I<sup>2</sup>aas have found success as turn mimics for biological applications.<sup>13,17</sup> This section summarizes information gained recently from structure-activity studies as

well as prototypes that have arrived from using I<sup>2</sup>aa residues to study the ideal spatial arrangements of the peptide backbone and side chains for binding and biological activity at various receptor targets.

#### 4.1. Enzyme inhibitors

##### 4.1.1. THROMBIN INHIBITORS

A trypsin-like serine protease, thrombin plays a key role in blood coagulation. Inhibition of the mechanism of action of thrombin has become a major goal for development of therapies of thrombotic disorders.<sup>17</sup> The D-Phe-Pro-Arg sequence has served as a starting point for the rational design of many thrombin inhibitors, such as D-Phe-Pro-Arg-CH<sub>2</sub>Cl.<sup>48</sup> Employing (3*R*)- and (3*S*)-3-benzyl-3-*N*-(Boc)amino-indolizidin-2-one-9-carboxylic acids **100**<sup>49</sup> as constrained Phe-Pro mimics, benzothiazole amino ketones (3*R*)- and (3*S*)-**102** were respectively prepared by coupling to amino alcohol **101** using EDC and HOBT, followed by alcohol oxidation with the Dess-Martin periodinane, and Boc group removal (Scheme 11).<sup>50</sup>



**Scheme 11.** Synthesis of indolizidinone thrombin inhibitors (3*R*)- and (3*S*)-**102**.

Both (3*R*)- and (3*S*)-**102** inhibited thrombin *in vitro* with *K<sub>i</sub>* values of 0.85 and 10 nM respectively. The configuration corresponding to D-phenylalanine at the P3 site was suggested to be optimal for binding to thrombin, because (3*R*)-**102** was greater than 10-fold more potent than its (3*S*)-**102** counterpart. When tested *in vitro* for potency at blocking coagulation and inhibiting anticoagulation enzymes, I<sup>2</sup>aa analog (3*R*)-**102** was greater than 1000-fold more selective for thrombin relative to other anticoagulation enzymes. In the arterio-venous shunt thrombosis model in baboons, (3*R*)-**102** was effective at 1 μg/min in blocking platelet deposition. Evaluation of (3*R*)-**102** *in vitro* and *in vivo* in both rat and primate models indicated good oral bioavailability, but low trans-epithelial permeability. Considering that mimicry of the β-strand secondary structure by I<sup>2</sup>aa analog (3*R*)-**102** was responsible for potent thrombin inhibition, potential exists for employing this approach to make inhibitors of other proteases that recognize β-strand motifs.<sup>50</sup>

##### 4.1.2. STAT3 INHIBITORS

Signal transducer and activator of transcription 3 (STAT3) is a transcription factor encoded by the *STAT3* gene. Phosphorylation of the STAT3 protein by receptor-associated kinases leads to dimerization and translocation to the cell nucleus, where it acts as a transcription activator. Involved in aberrant growth and survival signals in malignant tumor cells, STAT3 is a validated target for anticancer drug design. Employing I<sup>2</sup>aa and related heterocycle peptide mimics to study the bound conformation of a lead phosphopeptide [Ac-pTyr-Leu-Pro-Gln-Thr-Val-NH<sub>2</sub>], the structural requirements were examined for targeting the SH2 domain of STAT3 and preventing docking of cytokine and growth factor receptors responsible for signaling. Based on computational studies with the AUTODOCK program, the Leu-Pro sequence was replaced by I<sup>2</sup>aa residues in a set of phosphopeptides, which were synthesized using Fmoc-based solid phase peptide synthesis with Fmoc-I<sup>2</sup>aa on both Rink and Wang resin. Incorporation of (3*S*,6*S*,9*S*)- and (3*S*,6*R*,9*R*)-I<sup>2</sup>aa into Ac-pTyr-Leu-Pro-Gln-Thr-Val-NH<sub>2</sub> caused respectively 5- and 33-fold losses in

affinity compared to the parent phosphopeptide. Similarly, replacement of these I<sup>2</sup>aa residues for Leu-Pro in 4-phosphoryloxycinnamyl-Leu-Pro-Gln-Thr-Val-NH<sub>2</sub> resulted respectively in 4- and >400-fold reduced affinity. The resulting Ac-pTyr-(3*S*,6*S*,9*S*)-I<sup>2</sup>aa-Gln-Thr-Val-NH<sub>2</sub> and 4-phosphoryloxycinnamyl-(3*S*,6*S*,9*S*)-I<sup>2</sup>aa-Gln-Thr-Val-NH<sub>2</sub> analogs exhibited respectively 3530 ± 270 and 604 ± 68 nM affinities for STAT3.<sup>51,52</sup>

## 4.2. Receptor ligands

### 4.2.1. CCK RECEPTOR LIGANDS

Amino indolizidinone dicarboxylate **86** (Scheme 9) has been used to replace the Nle-Asp moiety in the CCK/opioid chimeric peptide Tyr-Nle-Gly-Trp-Nle-Asp-Phe-NH<sub>2</sub> to provide mimic **103** (Figure 10). Removal of the benzyl and Cbz groups by hydrogenation, and amine protection with an Fmoc group gave a building block for Fmoc/*t*-Bu solid phase peptide synthesis. After resin cleavage and protecting group removal with acid, the methyl ester was saponified using LiOH in H<sub>2</sub>O/MeOH and the resulting peptide mimic **103** was tested at the opioid and CCK receptors. Mimic **103** exhibited weak activity at both the δ- and μ-opioid receptors, and lost activity at the CCK receptors.<sup>31</sup>

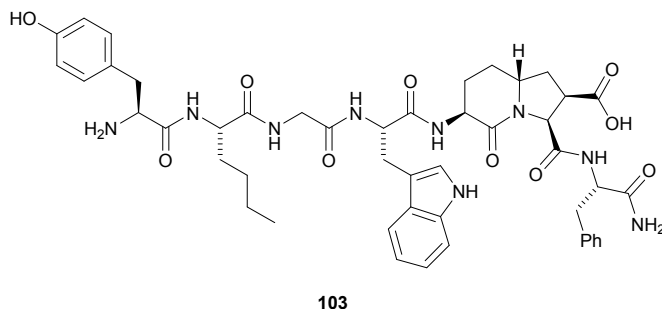


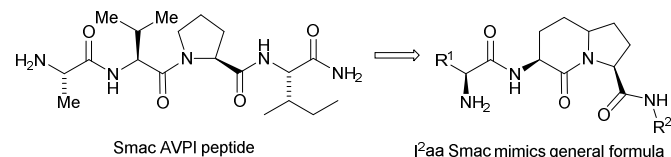
Figure 10. Constrained CCK/opioid chimeric peptide **103**.

### 4.2.2. SMAC MIMETICS

Second mitochondria-derived activator of caspase (Smac) or direct inhibitor of apoptosis protein (IAP) binding protein with low pI (Smac/DIABLO) is a pro-apoptotic protein released from mitochondria in response to apoptotic stimuli. Inhibition of caspases by IAPs is hypothesized to involve binding to their BIR3 domains. By binding competitively to the BIR3 domain through the N-terminal four-residue domain Ala-Val-Pro-Ile, Smac can liberate caspases.<sup>53</sup> To develop anticancer agents, Smac mimics have thus been pursued based on the Ala-Val-Pro-Ile tetra-peptide. Computational models based on the crystal structure of Smac protein in complex with the BIR3 domain of X-linked inhibitor of apoptosis protein (XIAP) revealed that the hydrophobic side chain of Ile<sup>4</sup> inserts into a hydrophobic pocket and its carbonyl group has no specific interactions with the protein.

The Val-Pro dipeptide has been replaced by I<sup>2</sup>aas in a series of analogs in which Ala<sup>1</sup> was also substituted with other aliphatic amino acid residues, and Ile<sup>4</sup> was replaced by benzyl and diphenylmethyl amines. The potency exhibited by the I<sup>2</sup>aa analogs **104-109** as inhibitors of IAP binding (Table 2) provided information on the conformation and structural requirements for affinity to the XIAP BIR3 domain as well as prototypes for developing anticancer therapeutics.<sup>54-57</sup>

Table 2. Smac Mimetics and Their Binding Affinities to XIAP BIR3.



Compound	R <sup>1</sup>	R <sup>2</sup>	K <sub>i</sub> ± SD, μM	Rate K <sub>i</sub> /K <sub>i</sub> <sub>AVPI</sub>	Ref
(6 <i>S</i> )- <b>104</b>	Me	Bn	4.47 ± 0.65	7.7	<sup>55</sup>
(6 <i>R</i> )- <b>104</b>	Me	Bn	> 100	n/a	<sup>55</sup>
(6 <i>S</i> )- <b>105</b>	Et	Bn	1.41 ± 0.16	2.4	<sup>54</sup>
(6 <i>S</i> )- <b>106</b>	<i>n</i> -Pr	Bn	> 100	n/a	<sup>54</sup>
(6 <i>S</i> )- <b>107</b>	<i>i</i> -Pr	Bn	43.11 ± 1.51	74.3	<sup>54</sup>
(6 <i>S</i> )- <b>108</b>	Me	CH(Ph) <sub>2</sub>	2.33 ± 0.68	4.0	<sup>57</sup>
(6 <i>S</i> )- <b>109</b>	Et	CH(Ph) <sub>2</sub>	0.35 ± 0.01	0.6	<sup>57</sup>

The binding affinities of the tested I<sup>2</sup>aa analogs (Table 2) were compared with binding affinity of AVPI peptide K<sub>i</sub><sub>AVPI</sub> = 0.58 ± 0.15 μM for the XIAP BIR3 domain. The binding affinity data demonstrated that the concave (6*S*)-I<sup>2</sup>aa analogs bound better than convex (6*R*)-counterparts. Although 2-aminobutyric acid (Abu) was a favorable replacement for Ala<sup>1</sup>, amino acids with branched side chains (e.g., Val and Leu) were not accommodated effectively for binding. Replacement of the benzyl amide of **105** by its diphenylmethyl counterpart gave a 4 fold enhancement in binding affinity producing the potent inhibitor Abu-I<sup>2</sup>aa-NHCH(Ph)<sub>2</sub> (**109**, K<sub>i</sub> = 0.35 ± 0.01 μM).

With a series of small-molecule Smac mimics targeting the XIAP BIR3 domain, binding affinities were evaluated by different predictive computational methods, including scoring functions (X-Score, Drugscore and M-Score) and MM-GBSA (molecular mechanics and generalized Born surface area). Although all four computational methods yielded poor to modest predictions for binding affinities, the MM-GBSA method provided several advantages over the other methods and considered the dominant contribution to the binding affinity to the XIAP BIR3 domain to be van der Waals interactions. Later efforts to include the ligand reorganization free energy in the MM-GBSA calculation improved the prediction of binding affinity so that it was consistent with information on ligand structure. The Smac mimic ligands were shown to adopt β-turn conformations similar to that observed in the crystal structure for the AVPI peptide-receptor complex.<sup>58</sup>

### 4.2.3. PROSTAGLANDIN F2α ALLOSTERIC MODULATORS

Prostaglandins are implicated in a number of biological events dictated by tissue specificity and mediated by their G-protein coupled receptors (GPCRs). The prostaglandin F2α (PGF2α) receptor (FP) was targeted to develop labour-suppressing drugs (tocolytics) that inhibit uterine contractions, because this GPCR is overexpressed in uterine tissue during labour. Employing the all D-amino acid peptide ilghrdyck as a lead, which exhibited non-competitive inhibitory activity against uterine contractions in the mouse model, (3*S*,6*S*,9*S*)-indolizidinone analogs (e.g., **110** and **111**, Figure 11) were developed which caused respective decreases in both basal and induced uterine contractions. For example, in pregnant mice, **110** delayed induced delivery with mean times up to 42 h.<sup>59-61</sup> Subsequently, the mechanism of action for **110** was demonstrated to involve allosteric modulation of FP contingent on PGF2α binding, and biased signaling that respectively increased ERK1/2 activity

and inhibited Rho-dependent actin remodeling and myometrial cell contraction by way of the GRq- and GR12-mediated pathways.

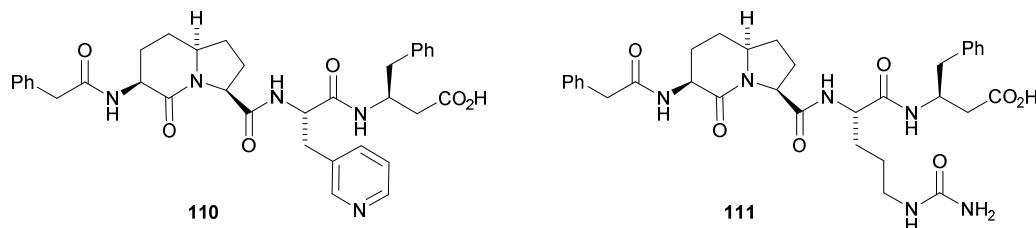
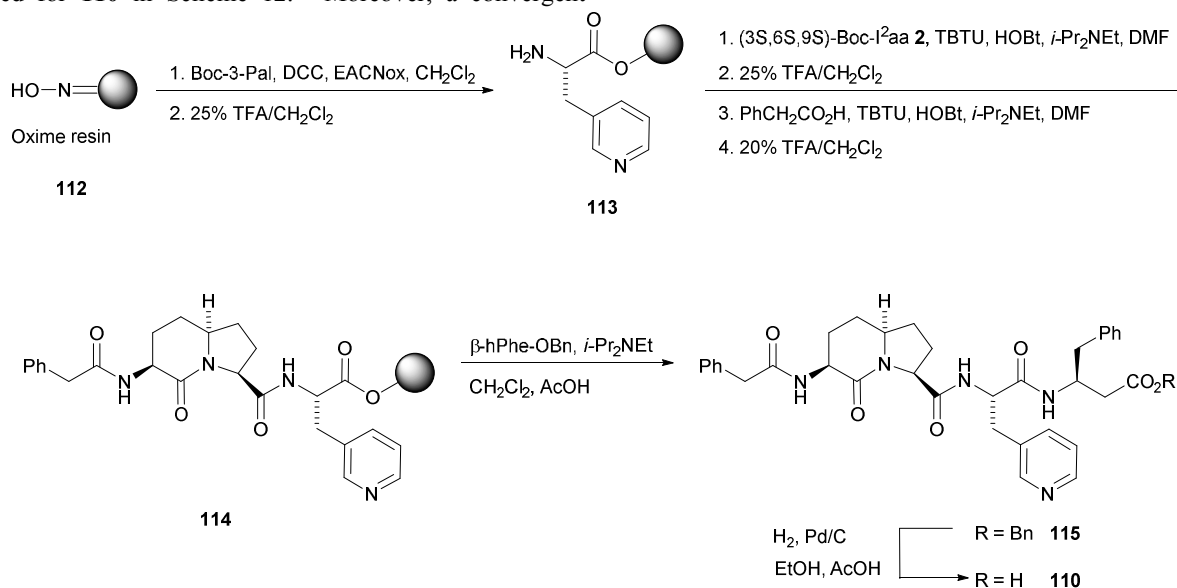


Figure 11. Azabicycloalkanone mimics **110** and **111**.

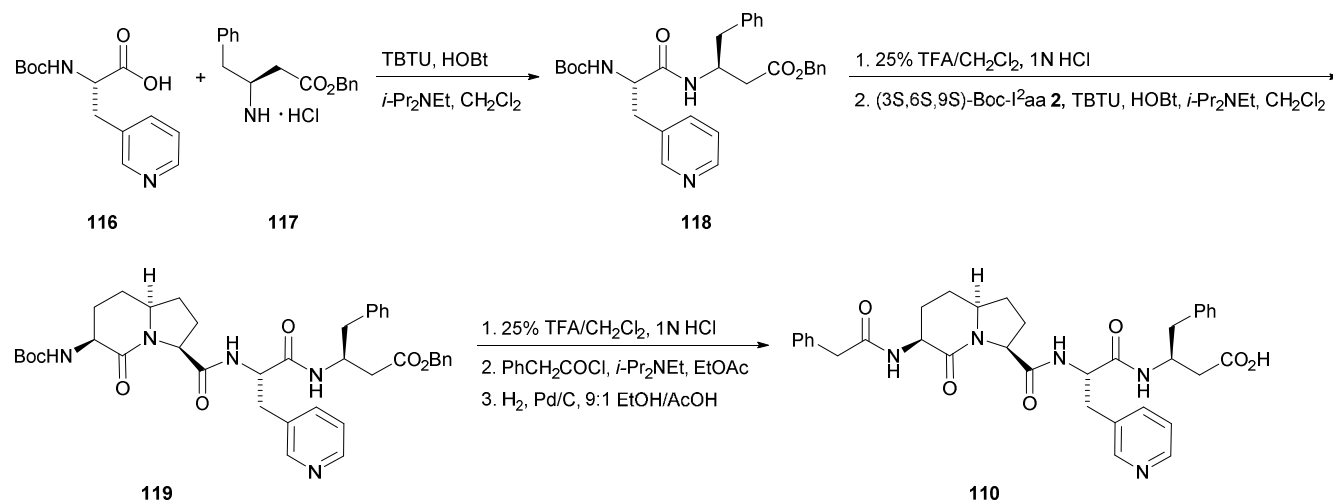
Indolizidinones **110** and **111** and their analogs were synthesized on solid support using a Boc strategy on oxime resin, as illustrated for **110** in Scheme 12.<sup>59</sup> Moreover, a convergent solution-phase method was developed to prepare **110** on a larger scale (Scheme 13).<sup>62</sup>



Scheme 12. Solid-supported synthesis of **110**.

The 3-phenylacetamido indolizidin-2-one 9-carboxyl and pyridinylalaninyl- $\beta$ -homophenylalanine sections of **110** are hypothesized to mimic respectively the active  $\beta$ -turn geometry about the Gly-His residue and the signaling pharmacophore of the Arg-Asp-Tyr triad in the parent peptide. The importance of

the stereochemistry of **111** was evidenced by the synthesis its enantiomer and (3*R*,6*R*,9*R*)-indolizidinone diastereomer, which in contrast to the active parent isomer, were inactive in the myometrial contraction assay.<sup>60</sup>

Scheme 13. Solution-phase synthesis of **110**.

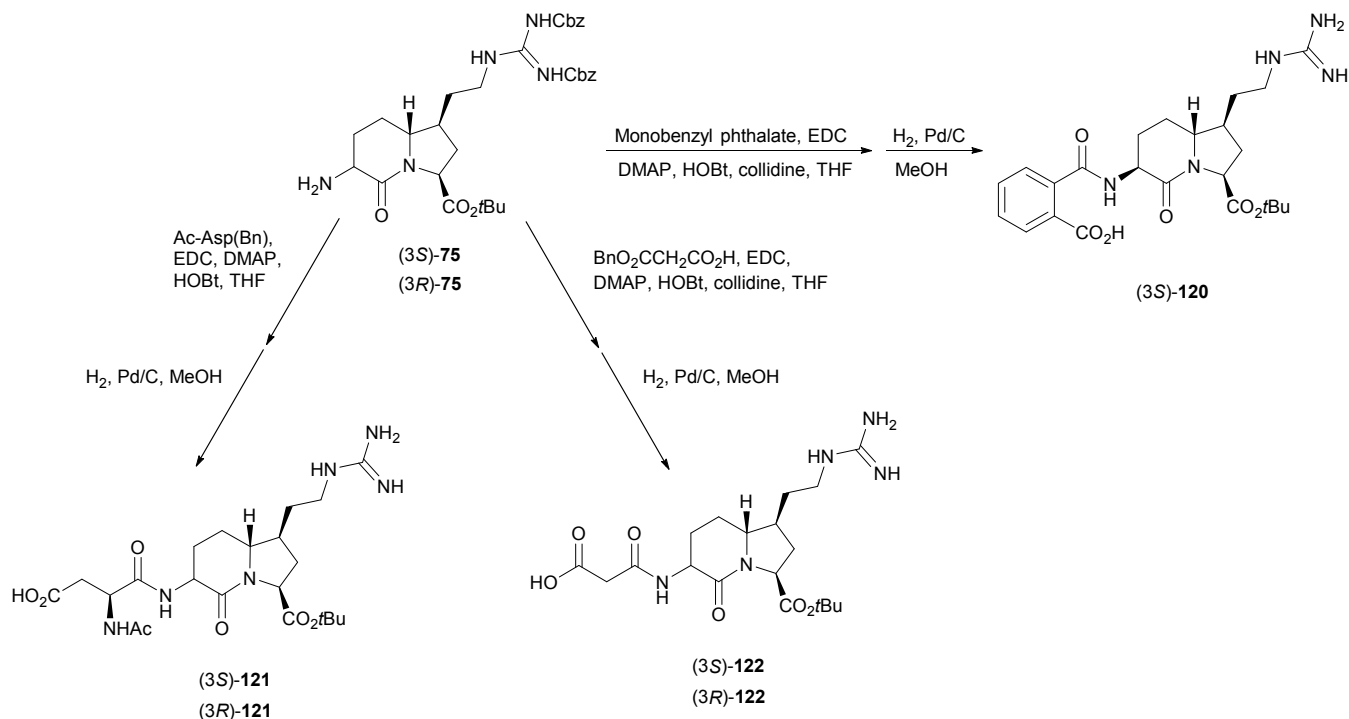
The development of indolizidinones such as **110** and **111** has provided important probes for studying mechanisms underlying parturition, as well as prototypical biased, allosteric modulators of FP for the design of improved selective tocolytic drugs.

#### 4.2.4. INTEGRIN RECEPTOR LIGANDS

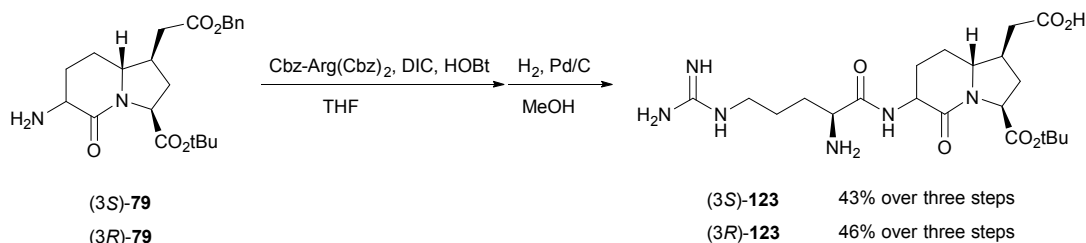
Integrin receptors are transmembrane-spanning proteins that participate in cell-matrix interactions in normal and malignant cell types. Serving in cell adhesion, integrin receptors bind to specific amino acid sequences, such as Arg-Gly-Asp. Selective antagonists of  $\alpha_v\beta_3$  and  $\alpha_v\beta_5$  integrin receptors have become promising targets for blocking tumor-induced angiogenesis.

In attempts to explore the conformational requirements for integrin affinity, 7-position substituted I<sup>2</sup>aa analogs bearing guanidino ethyl (e.g., **120-122**) and acetate (e.g., **123**) groups have been employed to synthesize constrained mimics of the Arg-Gly-Asp sequence.<sup>30</sup> The protected Gly-Arg and Gly-Asp

mimics **75** and **79** were respectively selectively acylated at the 3-position amine to provide constrained analogs **120-123** (Schemes 14 and 15). When linear RGD mimics **120-123** were examined in a competitive *in vitro* integrin-binding assay on purified  $\alpha_v\beta_3$  and  $\alpha_v\beta_5$  receptors, only **123** exhibited receptor affinity: (3*S*)- and (3*R*)-**123** bound  $\alpha_v\beta_3$  respectively at 0.3 and 2.6  $\mu\text{M}$  and  $\alpha_v\beta_5$  at 1.0 and 1.5  $\mu\text{M}$ . To better understand the experimental results, analogs **120-123** were docked into a model derived from the X-ray structure of the  $\alpha_v\beta_3$  integrin receptor. In the computational analysis, the I<sup>2</sup>aa bicycle was suggested to occupy a shallow cleft of the receptor; however, insufficient ligand length and conformational rigidity prevented the combination of both an Asp carboxylate and the Arg guanidino side chain from making electrostatic interactions respectively with the metal ion of the  $\beta$  subunit, and the negatively charged side chains of Asp<sup>150</sup> and Asp<sup>218</sup> in the  $\alpha$  subunit.<sup>30</sup>



Scheme 14. Synthesis of constrained RGD analogs **120-122**.



Scheme 15. Synthesis of integrin ligand **123**.

Cilengitide, cyclo[Arg-Gly-Asp-D-Phe-(*N*-Me)Val] blocks effectively the  $\alpha_v\beta_3$ ,  $\alpha_v\beta_5$ , and  $\alpha_5\beta_1$  integrin receptors, which play important roles in human tumor metastasis and tumor-induced angiogenesis, and has recently been in clinical trials for the treatment of glioblastoma and other cancer types.<sup>63,64</sup> A

series of cilengitide analogs have been synthesized by replacement of the D-Phe-Val dipeptide with various indolizidinone amino acids (Figure 12). As discussed above, the conformation of these cilengitide analogs was significantly influenced by the stereochemistry of the I<sup>2</sup>aa residue.

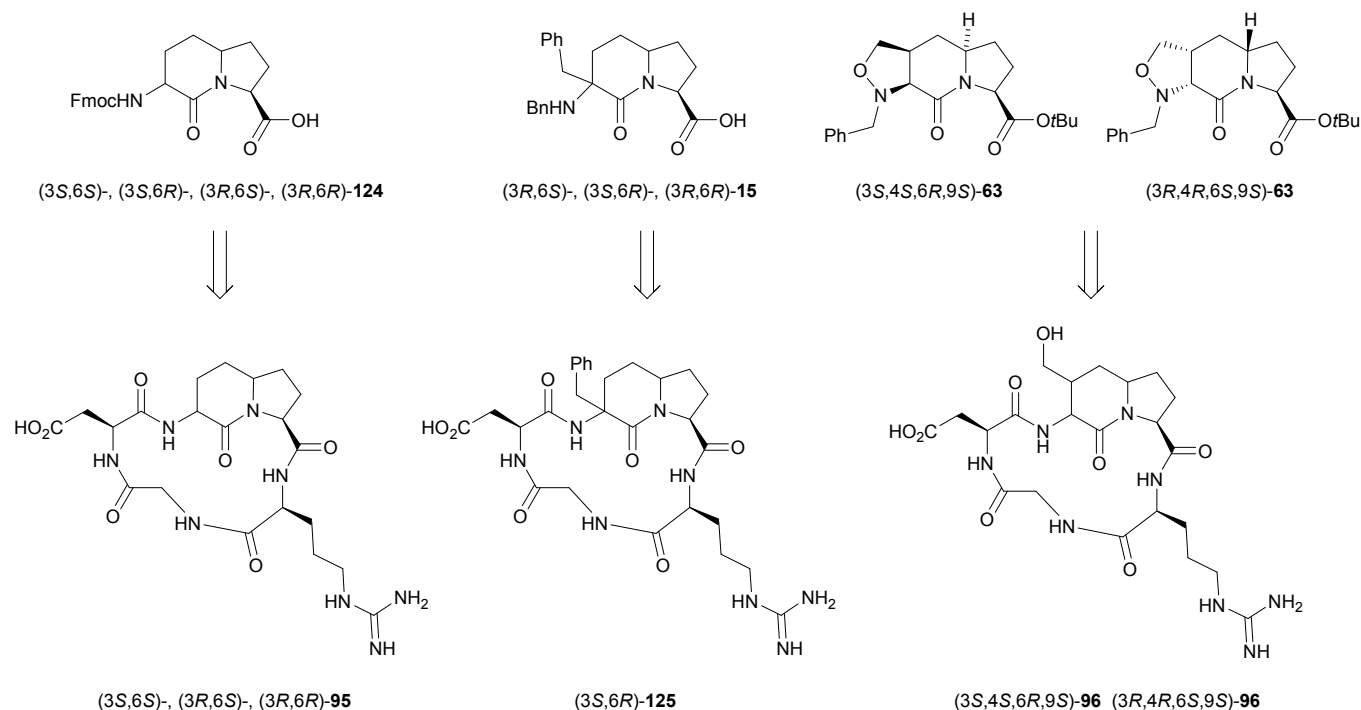
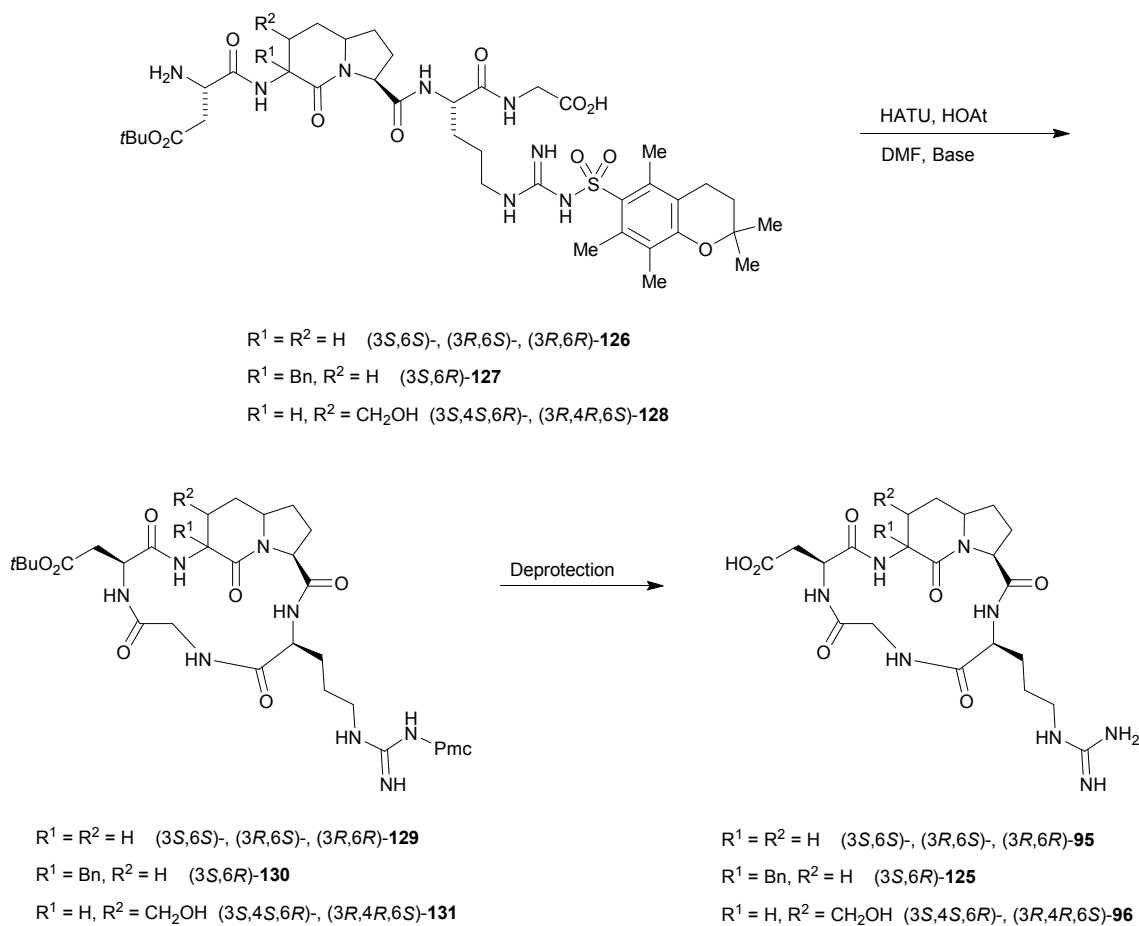


Figure 12. I<sup>2</sup>aa scaffolds and cyclo(Arg-Gly-Asp-I<sup>2</sup>aa) analogs.

Initially, three diastereomers of the parent I<sup>2</sup>aa residue were respectively introduced into cilengitide analogs using Fmoc-protection in a solid-phase approach on Super Acid Sensitive ResIN (SASRIN) to make the linear peptide sequence **126**. The cyclic peptides **129** were subsequently prepared by treatment of the protected linear peptide Asp(OtBu)-I<sup>2</sup>aa-Arg(Pmc)-Gly (**126**) with HATU and HOAt in solution, followed by removal of the protecting groups (Scheme 16).<sup>65</sup> 3-Benzyl I<sup>2</sup>aa **15** was replaced for D-Phe-Val in cilengitide analog **125** using a solution-phase approach commencing with glycine methyl ester and employing Cbz-protection. At the stage of the linear peptide, the methyl ester was converted to the corresponding

benzyl ester, which along with the terminal Cbz group was cleaved by hydrogenation to provide a precursor that was cyclized and deprotected as described for the I<sup>2</sup>aa analogs above.<sup>66</sup> Employing a similar solution-phase strategy 4-hydroxymethyl I<sup>2</sup>aa was introduced into cilengitide analogs (3S,4S,6R)-, and (3R,4R,6S)-**96** by way of its corresponding N-benzyl isoxazolidines (3S,4S,6R)-, and (3R,4R,6S)-**63**, which were cleaved and debenzylated by hydrogenolytic conditions prior to acylation with N-(Cbz)aspartate β-*tert*-butyl ester, cyclization and deprotection (Figure 12, Scheme 16).<sup>39</sup>



**Scheme 16.** Cyclization of linear I<sup>2</sup>aa peptides to make cilengitide analogs.

Cilengitide analogs (3*S*,6*S*)-, (3*R*,6*S*)-, and (3*R*,6*R*)-**95**,<sup>65,67</sup> (3*S*,6*R*)-**125**,<sup>66</sup> and (3*S*,4*S*,6*R*)-, and (3*R*,4*R*,6*S*)-**96**<sup>39</sup> were screened *in vitro* for ability to compete for the binding of <sup>125</sup>I-echistatin and biotinylated vitronectin to purified  $\alpha_v\beta_3$  and  $\alpha_v\beta_5$  integrin receptors (Table 3).

**Table 3.** Inhibition of <sup>125</sup>I-echistatin or biotinylated vitronectin binding to receptors for c(RGD-I<sup>2</sup>aa).

Compound	$\alpha_v\beta_3$		$\alpha_v\beta_5$
	IC <sub>50</sub> ± SD, nM	K <sub>i</sub> ± SD, nM	IC <sub>50</sub> ± SD, nM
c(RGDfV)	195.9 ± 16.8	157.8 ± 13.5	
(3 <i>S</i> ,6 <i>S</i> )- <b>95</b>	206.9 ± 8.7	191.0 ± 8.0	
(3 <i>R</i> ,6 <i>S</i> )- <b>95</b>	97.3 ± 7.5	89.8 ± 6.9	
(3 <i>R</i> ,6 <i>R</i> )- <b>95</b>	14.3 ± 4.7	11.5 ± 3.8	
(3 <i>S</i> ,6 <i>S</i> )- <b>125</b>	787.1 ± 54.6		4.12 ± 1.1
(3 <i>S</i> ,6 <i>R</i> )- <b>125</b>	75.7 ± 1.6		325.6 ± 20.3
(3 <i>S</i> ,4 <i>S</i> ,6 <i>R</i> )- <b>96</b> *	1816 ± 612		> 10 000
(3 <i>R</i> ,4 <i>R</i> ,6 <i>S</i> )- <b>96</b> *	53.7 ± 17.3		205 ± 33.5

\* Competition for biotinylated vitronectin was examined.

I<sup>2</sup>aa analog (3*R*,6*R*)-**95** showed the highest affinity to  $\alpha_v\beta_3$  and inhibited echistatin binding to  $\alpha_v\beta_3$  with an IC<sub>50</sub> of 14.3 ± 4.7 nM and a K<sub>i</sub> of 11.5 ± 3.8 nM (Table 3). The affinity of the (3*S*,6*R*)-3-benzyl-I<sup>2</sup>aa analog (3*S*,6*R*)-**125** was 10 fold higher for the  $\alpha_v\beta_3$  integrin (75.7 ± 1.6 nM IC<sub>50</sub> for  $\alpha_v\beta_3$ , and 325.6 ± 20.3 nM IC<sub>50</sub> for  $\alpha_v\beta_5$ ) than the affinity of its (3*S*,6*S*)-isomer

(3*S*,6*S*)-**125** (787.1 ± 54.6 nM IC<sub>50</sub> for  $\alpha_v\beta_3$ , and 4.12 ± 1.1 nM IC<sub>50</sub> for  $\alpha_v\beta_5$ ).<sup>68</sup> In the examination of the 4-hydroxymethyl-I<sup>2</sup>aa analogs (3*S*,4*S*,6*R*)-, and (3*R*,4*R*,6*S*)-**96**, the (3*R*,4*R*,6*S*)-isomer **96** exhibited the highest affinity in an *in vitro* assay measuring competitive binding of biotinylated vitronectin for purified  $\alpha_v\beta_3$  and  $\alpha_v\beta_5$  receptors. The nanomolar-range affinity of 4-hydroxymethyl-I<sup>2</sup>aa analog (3*R*,4*R*,6*S*)-**96** toward  $\alpha_v\beta_3$  integrin suggested that this functionalized RGD cyclic peptide could be suitable for targeted drug delivery.<sup>39</sup> The anti-angiogenic and antitumor activity of compound (3*R*,4*R*,6*S*)-**96** were measured in cell adhesion assays on two cell models: human umbilical vein vascular endothelial cells (HUVEC) and bladder carcinoma cells (ECV-304). 4-Hydroxymethyl-I<sup>2</sup>aa analog (3*R*,4*R*,6*S*)-**96** inhibited significantly adhesion of both cell types to fibronectin and vitronectin in the micromolar range without cytotoxic activity.<sup>39</sup>

#### 4.2.5. FUNCTIONALIZATION AND CONJUGATED COMPLEXES OF INTEGRIN ANTAGONISTS

Employing cyclic Arg-Gly-Asp analogs containing the 4-azidomethyl-I<sup>2</sup>aa residue (e.g., **132**) a variety of bioconjugates have been prepared by CuAAC reactions on the azide,<sup>24,39,69-72</sup> as well as by reduction of the azide to an amine and subsequent acylation.<sup>69-74</sup> 4-Hydroxymethyl penta-peptide mimic (3*R*,4*R*,6*S*)-**96** was employed as starting material to make the azidomethyl analog **132** (Figure 13) for the bio-conjugations, because of its relatively high affinity for the  $\alpha_v\beta_3$  integrin receptor in *in vitro* binding assays (IC<sub>50</sub> of 53.7 ± 17.3 nM).

Conjugations were made to create fluorescent probes using fluorescein<sup>69</sup> and cyanine dyes,<sup>74</sup> to produce magnetic resonance imaging contrast agents with metal coordinating ligands such as DOTA for binding gadolinium,<sup>71</sup> to link alendronic acid as a bisphosphonate anchor for coating titanium implants and hydroxyapatite-like objects,<sup>72</sup> to attach taxane drugs (e.g., paclitaxel),<sup>70</sup> as well as to add thiols for subsequent attachment to gold nanoparticles.<sup>73</sup> A variety of linker strategies possessing various spacers, such as poly-ethylene glycol chains, were employed in these strategies, which have provided some high affinity and specific integrin receptor ligands with interesting potential for imaging and treating cancer.

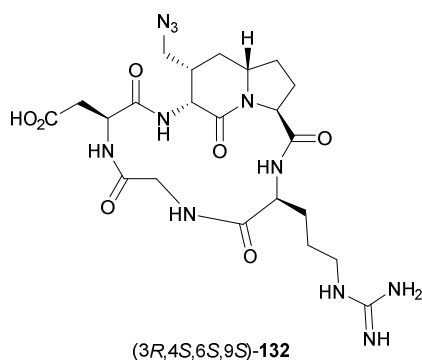


Figure 13. Azido-I<sup>2</sup>aa integrin ligand 132.

#### 4.2.6. CGRP RECEPTOR LIGANDS

Calcitonin gene-related peptide (CGRP, ACDTATCVTHRLAGLLSRGGVVKNNFVPTNVGSKAF-NH<sub>2</sub>, for  $\alpha$ -form) is a nervous system peptide, which exhibits many physiological influences including very potent vasodilatory effects with actions on the cardiovascular and central nervous systems, reproductive organs, skeletal muscles, calcium metabolism, insulin regulation, and gastric secretion. CGRP antagonists have been pursued as candidates for treating indications, such as non-insulin-dependent diabetes mellitus, migraine headache, pain, inflammation, and morphine-induced analgesia. Short C-terminal peptides derived from CGRP, such as [D<sup>31</sup>,P<sup>34</sup>,F<sup>35</sup>]CGRP<sub>27-37</sub> have exhibited significant antagonist activity. Scans of [D<sup>31</sup>,P<sup>34</sup>,F<sup>35</sup>]CGRP<sub>27-37</sub> and [D<sup>31</sup>,P<sup>34</sup>,F<sup>35</sup>]CGRP<sub>29-37</sub> were performed using (3S,6S,9S)-I<sup>2</sup>aa to identify turn conformations responsible for antagonist activity (Table 4).<sup>75</sup> Although most of the analogs exhibited no activity, replacement of Gly<sup>33</sup>-Pro<sup>34</sup> by the rigid dipeptide surrogate produced [D<sup>31</sup>,I<sup>2</sup>aa<sup>33,34</sup>,F<sup>35</sup>]CGRP<sub>27-37</sub> 139, which exhibited 7-fold enhanced activity relative to the parent peptide. A complementary relationship between the azabicycloalkane amino acid analog and its aza-Gly<sup>33</sup>-counterpart, [D<sup>31</sup>,aza-G<sup>33</sup>,P<sup>34</sup>,F<sup>35</sup>]CGRP<sub>27-37</sub> which exhibited 10-fold better activity than the parent peptide led to the hypothesis that a type II'  $\beta$ -turn centered at Gly<sup>33</sup>-Pro<sup>34</sup> was a structural requirement for the antagonist activity of the undecapeptide [D<sup>31</sup>P<sup>34</sup>F<sup>35</sup>]-CGRP<sub>27-37</sub> at the CGRP receptor.<sup>76</sup>

Table 4. Indolizidinone CGRP analogs and antagonist activity.

Compound	Peptides	Structure	pIC <sub>50</sub>
133	[D <sup>31</sup> ,P <sup>34</sup> ,F <sup>35</sup> ]CGRP <sub>27-37</sub>	FVPTDVGPF <sup>2</sup> AF-NH <sub>2</sub>	6.15 ± 0.18
134	[D <sup>31</sup> ,P <sup>34</sup> ,F <sup>35</sup> ]CGRP <sub>29-37</sub>	PTDVGPF <sup>2</sup> AF-NH <sub>2</sub>	6.11 ± 0.18
135	[I <sup>2</sup> aa <sup>31-32</sup> ,P <sup>34</sup> ,F <sup>35</sup> ]CGRP <sub>29-37</sub>	PTI <sup>2</sup> aaGPF <sup>2</sup> AF-NH <sub>2</sub>	N/A *
136	[D <sup>31</sup> ,I <sup>2</sup> aa <sup>34-35</sup> ]CGRP <sub>29-37</sub>	PTDVGI <sup>2</sup> aaAF-NH <sub>2</sub>	N/A
137	[I <sup>2</sup> aa <sup>31-32</sup> ,P <sup>34</sup> ,F <sup>35</sup> ]CGRP <sub>27-37</sub>	FVPTI <sup>2</sup> aaGPF <sup>2</sup> AF-NH <sub>2</sub>	N/A
138	[D <sup>31</sup> ,I <sup>2</sup> aa <sup>32-33</sup> ,P <sup>34</sup> ,F <sup>35</sup> ]CGRP <sub>27-37</sub>	FVPTDI <sup>2</sup> aaPFAF-NH <sub>2</sub>	N/A
139	[D <sup>31</sup> ,I <sup>2</sup> aa <sup>33-34</sup> ,F <sup>35</sup> ]CGRP <sub>27-37</sub>	FVPTDVI <sup>2</sup> aaFAF-NH <sub>2</sub>	6.97 ± 0.17
140	[D <sup>31</sup> ,I <sup>2</sup> aa <sup>34-35</sup> ]CGRP <sub>27-37</sub>	FVPTDVGI <sup>2</sup> aaAF-NH <sub>2</sub>	N/A

\* N/A - no inhibition was detected with peptide concentrations up to 100  $\mu$ M.

## Conclusions

A significant amount of research on the synthesis, conformational analysis and biological activity of indolizidin-2-one amino acids has been generated since this subject was last reviewed in 2004. In particular, new synthetic methods were developed to give access to I<sup>2</sup>aa analogs possessing substituents on the six-membered lactam. Incorporation of the parent ring system into cyclic peptides bearing the integrin receptor ligand Arg-Gly-Asp and conformational analysis by NMR spectroscopic and computational methods has provided insight into the influence of stereochemistry on the preferred orientation of the bicyclic ring system. Moreover, applications of the parent I<sup>2</sup>aa and substituted variants have provided enzyme inhibitors and receptor ligands. Information gleaned from studying the latter has aided understanding of the bioactive conformations of natural peptide ligands as well as insight for the better use of these mimics in structure-activity relationship studies. Moreover, several analogs have exhibited useful biological activity with potential for therapeutic applications, such as drugs and diagnostics to treat cancer, as well as inhibitors of uterine contractions to deter preterm labour. Paramount to the success of I<sup>2</sup>aa as a tool for studying the elements responsible for biological activity has been its utility in rigidifying backbone geometry to mimic natural peptide secondary structures, particularly turn conformers. The growing track record of success in applying these tools to study biological peptides, improved methods for their synthesis and introduction into peptide mimics, and enhanced understanding of their conformational preferences, all bear well for continued effective use of I<sup>2</sup>aa analogs in peptide science and medicinal chemistry.

## Acknowledgements

The authors would like to thank the Natural Sciences and Engineering Research Council of Canada (NSERC), the Canadian Institutes of Health Research (CIP-79848), the March of Dimes, and the Canadian Foundation for Innovation for financial support.

## Abbreviations

3-Pal, L-3-Pyridylalanine;  $\beta$ -hPhe, (S)-3-Amino-4-phenylbutyric acid; Abu, 2-Aminobutyric acid; Ac, Acetyl; BIR, Baculoviral inhibitor of apoptosis protein repeat; Bn, Benzyl; Boc, *tert*-Butyloxycarbonyl; Cbz, Carboxybenzyl (Carbobenzyloxy); CCK, Cholecystokinin; CGRP, Calcitonin gene-related peptide; CuAAC, Copper-Catalyzed Azide-Alkyne Cycloaddition; DBU, 1,8-Diazabicyclo[5.4.0]undec-7-ene; DCC, *N,N'*-Dicyclohexylcarbodiimide; DIC, *N,N'*-Diisopropylcarbodiimide; DMAP, 4-Dimethylaminopyridine; DMS, Dimethylsulfide; EACNox, Ethyl 2-(hydroxyimino)-2-

cianoacetate; EDC, *N*-(3-Dimethylaminopropyl)-*N'*-ethylcarbodiimide hydrochloride; Fmoc, 9-Fluorenylmethoxycarbonyl; FP, Prostaglandin-F2 $\alpha$  (PGF2 $\alpha$ ) receptor; GBSA, Generalized Born surface area; GPCR, G-protein coupled receptor; HATU, *O*-(7-azabenzotriazol-1-yl)-*N,N,N'*-tetramethyluronium hexafluorophosphate; hPhe, Homophenylalanine; HMDS, Hexamethyldisilazide [bis-(trimethylsilyl)amide]; HMPA, Hexamethylphosphoramide; HOAt, 1-Hydroxy-7-azabenzotriazole; HOBt, Hydroxybenzotriazole; I<sup>2</sup>aa, Indolizidin-2-one amino acid; IAP, Inhibitor of apoptosis protein; MM, Molecular mechanics; Mtr, 4-methoxy-2,3,6-trimethylbenzenesulphonyl; Nle, L-Norleucine; NOESY, Nuclear Overhauser effect spectroscopy; PDC, Pyridinium dichromate; PGF2 $\alpha$ , Prostaglandin F2 $\alpha$ ; Phth, Phthalyl; Pmc, 2,2,5,7,8-Pentamethylchroman-6-sulphonyl (sulfonyl); pTyr, Tyr(PO<sub>3</sub>H<sub>2</sub>) (phosphotyrosine); SD, Standard deviation; Smac, Second mitochondria-derived activator of caspase; STAT3, Signal transducer and activator of transcription 3; TBDMS, *tert*-Butyldimethylsilyl; TBDPS, *tert*-Butyldiphenylsilyl; TBTU, *O*-(Benzotriazol-1-yl)-*N,N,N'*-tetramethyluronium tetrafluoroborate; TDS, Thexyldimethylsilyl; TEMPO, (2,2,6,6-Tetramethylpiperidin-1-yl)oxy; TFA, Trifluoroacetic acid; XIAP, X-Linked inhibitor of apoptosis protein.

## Notes and references

<sup>a</sup> Département de Chimie, Université de Montréal, Montréal H3C 3J7, Canada

- Lubell, W. D. *Org. Lett.* **2012**, *14*, 4297.
- Gante, J. *Angew. Chem., Int. Ed. Engl.* **1994**, *33*, 1699.
- Hruby, V. J.; Balse, P. M. *Curr. Med. Chem.* **2000**, *7*, 945.
- Abell, A. D. *Lett. Pept. Sci.* **2002**, *8*, 267.
- Vagner, J.; Qu, H.; Hruby, V. J. *Curr. Opin. Chem. Biol.* **2008**, *12*, 292.
- Moradi, S.; Soltani, S.; Ansari, A. M.; Sardari, S. *Anti-Infect. Agents Med. Chem.* **2009**, *8*, 327.
- Kharb, R.; Rana, M.; Sharma, P. C.; Yar, M. S. *J. Chem. Pharm. Res.* **2011**, *3* (6), 173.
- Ko, E.; Liu, J.; Burgess, K. *Chem. Soc. Rev.* **2011**, *40*, 4411.
- Lienkamp, K.; Madkour, A. E.; Tew, G. N. *Adv. Polym. Sci.* **2013**, *251*, 141.
- Hruby, V. J.; Cai, M. *Annu. Rev. Pharmacol. Toxicol.* **2013**, *53*, 557.
- Jamieson, A. G.; Boutard, N.; Sabatino, D.; Lubell, W. D. *Chem. Biol. Drug Des.* **2013**, *81*, 148.
- Hanessian, S.; McNaughton-Smith, G.; Lombart, H.-G.; Lubell, W. D. *Tetrahedron* **1997**, *53*, 12789.
- Cluzeau, J.; Lubell, W. D. *Biopolymers* **2005**, *80*, 98.
- Blakeney, J. S.; Reid, R. C.; Le, G. T.; Fairlie, D. P. *Chem. Rev.* **2007**, *107*, 2960.
- The ring system numbering was used as in review<sup>12</sup> to conveniently discuss the heterocyclic system, albeit it does not necessarily conform to IUPAC standards.
- Halab, L.; Gosselein, F.; Lubell, W. D. *Biopolymers* **2000**, *55*, 101.
- Belvisi, L.; Colombo, L.; Manzoni, L.; Potenza, D.; Scolastico, C. *Synlett* **2004**, *9*, 1449.
- Maison, W.; Prenzel, A. H. G. P. *Synthesis* **2005**, *7*, 1031.
- Mandal, P. K.; Kaluarachchi, K. K.; Ogrin, D.; Bott, S. G.; McMurray, J. S. *J. Org. Chem.* **2005**, *70*, 10128.
- Manzoni, L.; Belvisi, L.; Colombo, M.; Di Carlo, E.; Forni, A.; Scolastico, C. *Tetrahedron Lett.* **2004**, *45*, 6311.
- Manzoni, L.; Belvisi, L.; Di Carlo, E.; Forni, A.; Invernizzi, D.; Scolastico, C. *Synthesis* **2006**, *7*, 1133.
- Bravin, F. M.; Busnelli, G.; Colombo, M.; Gatti, F.; Manzoni, L.; Scolastico, C. *Synthesis* **2004**, *3*, 353.
- Manzoni, L.; Arosio, D.; Belvisi, L.; Bracci, A.; Colombo, M.; Invernizzi, D.; Scolastico, C. *J. Org. Chem.* **2005**, *70*, 4124.
- Arosio, D.; Bertoli, M.; Manzoni, L.; Scolastico, C. *Tetrahedron Lett.* **2006**, *47*, 3697.
- Kaul, R.; Surprenant, S.; Lubell, W. D. *J. Org. Chem.* **2005**, *70*, 3838.
- Kaul, R.; Surprenant, S.; Lubell, W. D. *J. Org. Chem.* **2005**, *70*, 4901.
- Godina, T. A.; Lubell, W. D. *J. Org. Chem.* **2011**, *76*, 5846.
- Surprenant, S.; Lubell, W. D. *Org. Lett.* **2006**, *8*, 2851.
- Artale, E.; Banfi, G.; Belvisi, L.; Colombo, L.; Colombo, M.; Manzoni, L.; Scolastico, C. *Tetrahedron* **2003**, *59*, 6241.
- Manzoni, L.; Bassanini, M.; Belvisi, L.; Motto, I.; Scolastico, C.; Castorina, M.; Pisano, C. *Eur. J. Org. Chem.* **2007**, *8*, 1309.
- Ndungu, J. M.; Cain, J. P.; Davis, P.; Ma, S.-W.; Vanderah, T. W.; Lai, J.; Porreca, F.; Hruby, V. J. *Tetrahedron Lett.* **2006**, *47*, 2233.
- Hanessian, S.; Papeo, G.; Fettes, K.; Therrien, E.; Viet, M. T. P. *J. Org. Chem.* **2004**, *69*, 4891.
- Hanessian, S.; Sables, H.; Munro, A.; Therrien, E. *J. Org. Chem.* **2003**, *68*, 7219.
- Lombart, H.-G.; Lubell, W. D. *J. Org. Chem.* **1996**, *61*, 9437.
- Polyak, F.; Lubell, W. D. *J. Org. Chem.* **1998**, *63*, 5937.
- Polyak, F.; Lubell, W. D. *J. Org. Chem.* **2001**, *66*, 1171.
- Belvisi, L.; Bernardi, A.; Colombo, M.; Manzoni, L.; Potenza, D.; Scolastico, C.; Giannini, G.; Marcellini, M.; Riccioni, T.; Castorina, M.; LoGiudice, P.; Pisano, C. *Bioorg. Med. Chem.* **2006**, *14*, 169.
- Potenza, D.; Belvisi, L. *Org. Biomol. Chem.* **2008**, *6*, 258.
- Manzoni, L.; Belvisi, L.; Arosio, D.; Civera, M.; Pilkington-Miksa, M.; Potenza, D.; Caprini, A.; Araldi, E. M. V.; Monferini, E.; Mancino, M.; Podest, F.; Scolastico, C. *ChemMedChem* **2009**, *4*, 615.
- Khiat, A.; Fournier, A.; Lubell, W.; Boulanger, Y. *J. Cardiovasc. Pharmacol.* **2000**, *36* (Suppl. 1), S33.
- Soave, R.; Destro, R. *Acta Crystallogr., Sect. C: Cryst. Struct. Commun.* **2002**, *C58*, o507.
- Ball, J. B.; Alewood, P. F. *J. Mol. Recognit.* **1990**, *3*, 55.
- Madison, V.; Kopple, K. D. *J. Am. Chem. Soc.* **1980**, *102*, 4855.
- Glenn, M.P.; Fairlie, D.P. *Mini-Rev. Med. Chem.* **2002**, *2*, 433.
- Loughlin, W.A.; Tyndall, J.D.A.; Glenn, M.P.; Fairlie, D.P. *Chem. Rev.* **2004**, *104*, 6085.
- Henchey, L.K.; Jochim, A.L.; Arora, P.S. *Curr. Opin. Chem. Biol.* **2008**, *12*, 692.
- Bullock, B.N.; Jochim, A.L.; Arora, P.S. *J. Am. Chem. Soc.* **2011**, *133*, 14220.
- Kettner, C.; Shaw, E. *Thromb. Res.* **1979**, *14*, 969.
- Eguchi, M.; Kim, H.-O.; Gardner, B. S.; Boatman, P. D.; Lee, M. S.; Nakanishi, H.; Kahn, M. In *Peptides: Frontiers of Peptide Science*, Proceedings of the Fifteenth American Peptide Symposium, Nashville, Tennessee, June 14-19, 1997; Tam, J. P., Kaumaya, P. T.

- P., Eds.; Kluwer Academic Publishers: Dordrecht, The Netherlands, 1998; p 212.
50. Boatman, P. D.; Ogbu, C. O.; Eguchi, M.; Kim, H.-O.; Nakanishi, H.; Cao, B.; Shea, J. P.; Kahn, M. *J. Med. Chem.* **1999**, *42*, 1367.
51. Mandal, P. K.; Limbrick, D.; Coleman, D. R.; Dyer, G. A.; Ren, Z.; Birtwistle, J. S.; Xiong, C.; Chen, X.; Briggs, J. M.; McMurray, J. S. *J. Med. Chem.* **2009**, *52*, 2429.
52. Dhanik, A.; McMurray, J. S.; Kavraki, L. E. *PLoS One* **2012**, *7*, e51603.
53. Wu, G.; Chai, J.; Suber, T. L.; Wu, J.-W.; Du, C.; Wang, X.; Shi Y. *Nature* **2000**, *408*, 1008.
54. Sun, H.; Nikolovska-Coleska, Z.; Yang, C.-Y.; Xu, L.; Tomita, Y.; Krajewski, K.; Roller, P. P.; Wang, S. *J. Med. Chem.* **2004**, *47*, 4147.
55. Sun, H.; Nikolovska-Coleska, Z.; Yang, C.-Y.; Xu, L.; Liu, M.; Tomita, Y.; Pan, H.; Yoshioka, Y.; Krajewski, K.; Roller, P. P.; Wang, S. *J. Am. Chem. Soc.* **2004**, *126*, 16686.
56. Sharma, S. K.; Straub, C.; Zawel, L. *Int. J. Pept. Res. Ther.* **2006**, *12*, 21.
57. Sun, H.; Stuckey, J. A.; Nikolovska-Coleska, Z.; Qin, D.; Meagher, J. L.; Qiu, S.; Lu, J.; Yang, C.-Y.; Saito, N. G.; Wang, S. *J. Med. Chem.* **2008**, *51*, 7169.
58. Yang, C.-Y.; Sun, H.; Chen, J.; Nikolovska-Coleska, Z.; Wang, S. *J. Am. Chem. Soc.* **2009**, *131*, 13709.
59. Bourguet, C. B.; Hou, X.; Chemtob, S.; Lubell, W. D. *Peptides* **2006**, 436.
60. Bourguet, C. B.; Hou, X.; Chemtob, S.; Lubell, W. D. *Adv. Exp. Med. Biol.* **2009**, *611*, 271.
61. Goupil, E.; Tassy, D.; Bourguet, C.; Quiniou, C.; Wisheart, V.; Petrin, D.; Le Gouill, C.; Devost, D.; Zingg, H. H.; Bouvier, M.; Saragovi, H. U.; Chemtob, S.; Lubell, W. D.; Claing, A.; Hébert, T. E.; Laporte, S. A. *J. Biol. Chem.* **2010**, *285*, 25624.
62. Bourguet, C. B.; Goupil, E.; Tassy, D.; Hou, X.; Thouin, E.; Polyak, F.; Hébert, T. E.; Claing, A.; Laporte, S. A.; Chemtob, S.; Lubell, W. D. *J. Med. Chem.* **2011**, *54*, 6085.
63. Reardon, D. A.; Nabors, L. B.; Stupp, R.; Mikkelsen, T. *Expert Opin. Invest. Drugs* **2008**, *17*, 1225.
64. Mas-Moruno, C.; Rechenmacher, F.; Kessler, H. *Anti-Cancer Agents Med. Chem.* **2010**, *10*, 753.
65. Belvisi, L.; Bernardi, A.; Checchia, A.; Manzoni, L.; Potenza, D.; Scolastico, C.; Castorina, M.; Cupelli, A.; Giannini, G.; Carminati, P.; Pisano C. *Org. Lett.* **2001**, *3*, 1001.
66. Arosio, D.; Belvisi, L.; Colombo, L.; Colombo, M.; Invernizzi, D.; Manzoni, L.; Potenza, D.; Serra, M.; Castorina, M.; Pisano, C.; Scolastico, C. *ChemMedChem* **2008**, *3*, 1589.
67. Belvisi, L.; Riccioni, T.; Marcellini, M.; Vesci, L.; Chiarucci, I.; Efrati, D.; Potenza, D.; Scolastico, C.; Manzoni, L.; Lombardo, K.; Stasi, M. A.; Orlandi, A.; Ciucci, A.; Nico, B.; Ribatti, D.; Giannini, G.; Presta, M.; Carminati, P.; Pisano, C. *Mol. Cancer Ther.* **2005**, *4*, 1670.
68. Belvisi, L.; Caporale, A.; Colombo, M.; Manzoni, L.; Potenza, D.; Scolastico, C.; Castorina, M.; Cati, M.; Giannini, G.; Pisano, C. *Helv. Chim. Acta* **2002**, *85*, 4353.
69. Arosio, D.; Manzoni, L.; Araldi, E. M. V.; Caprini, A.; Monferini, E.; Scolastico, C. *Bioconjugate Chem.* **2009**, *20*, 1611.
70. Pilkington-Miksa, M.; Arosio, D.; Battistini, L.; Belvisi, L.; De Matteo, M.; Vasile, F.; Burreddu, P.; Carta, P.; Rasso, G.; Perego, P.; Carenini, N.; Zunino, F.; De Cesare, M.; Castiglioni, V.; Scanziani, E.; Scolastico, C.; Casiraghi, G.; Zanardi, F.; Manzoni, L. *Bioconjugate Chem.* **2012**, *23*, 1610.
71. Manzoni, L.; Belvisi, L.; Arosio, D.; Bartolomeo, M. P.; Bianchi, A.; Brioschi, C.; Buonsanti, F.; Cabella, C.; Casagrande, C.; Civera, M.; De Matteo, M.; Fugazza, L.; Lattuada, L.; Maisano, F.; Miragoli, L.; Neira, C.; Pilkington-Miksa, M.; Scolastico, C. *ChemMedChem* **2012**, *7*, 1084.
72. Drago, C.; Arosio, D.; Casagrande, C.; Manzoni, L. *ARKIVOC (Gainesville, FL, U. S.)* **2013**, *2*, 185.
73. Arosio, D.; Manzoni, L.; Araldi, E. M. V.; Scolastico, C. *Bioconjugate Chem.* **2011**, *22*, 664.
74. Lanzardo, S.; Conti, L.; Brioschi, C.; Bartolomeo, M. P.; Arosio, D.; Belvisi, L.; Manzoni, L.; Maiocchi, A.; Maisano, F.; Forni, G. *Contrast Media Mol. Imaging* **2011**, *6*, 449.
75. Boeglin, D.; Hamdan, F. F.; Melendez, R. E.; Cluzeau, J.; Laperriere, A.; Heroux, M.; Bouvier, M.; Lubell, W. D. *J. Med. Chem.* **2007**, *50*, 1401.
76. Bourguet, C. B.; Sabatino, D.; Lubell, W. D. *Biopolymers* **2008**, *90*, 824.